International Journal of Earth Sciences (2019) 108:2407–2428
https://doi.org/10.1007/s00531-019-01770-2

ORIGINAL PAPER

Pre-Mesozoic Crimea as a continuation of the Dobrogea platform: insights from detrital zircons in Upper Jurassic conglomerates, Mountainous Crimea

N. B. Kuznetsov[1,2,3] · E. A. Belousova[2] · W. L. Griffin[2] · S. Y. O'Reilly[2] · T. V. Romanyuk[2,4] · S. V. Rud'ko[1]

Received: 24 June 2019 / Accepted: 29 August 2019 / Published online: 10 September 2019

Abstract

U–Pb dating, Hf-isotope, and trace-element studies on two detrital zircon samples from sandstone interlayers in the Upper Jurassic conglomerates of the Southern coast of the Mountainous Crimea provide new information on the primary crystalline complexes from which those conglomerates were sourced. The U–Pb age spectra of studied zircons suggest that they were most likely sourced from the (meta)sedimentary complexes of the Eastern and Western Pontides blocks and the Dobrogea platform. In particular, a close similarity of the Precambrian age spectra with the detrital zircons from Late Neoproterozoic–Late Paleozoic (meta)sedimentary complexes of the Dobrogea block provides strong supporting evidence for the affinity between the Pre-Mesozoic basement of the Crimea and the Dobrogea platform. The zircons in the first sample were recycled through Dobrogea sedimentary complexes and originated from terranes with Amazonia affinities, while zircons in the second sample were recycled through the Taurides and originated from terranes related to northeastern Africa and Arabia. The strong similarity of the Precambrian parts of the age spectra of the Dobrogea complexes and the sample K15-007 suggests a resemblance of the Crimea's Pre-Mesozoic foundation and the Dobrogea platform. Initial analytical data are provided in Electronic Supplementary Materials A (ESM A). Descriptions of measurement parameters, methodologies, and constants used to process primary analytical data and some processing results are reported in ESM B (Figs. B1–B8). Schemes of locations within Balkans–Anatolia–Black Sea–Caucasus region the crystalline complexes with Jurassic, Triassic, Permian–Carboniferous, as well as Late Neoproterozoic–Cambrian and Ordovician–Devonian ages are in ESM C (Figs. C1, C3–C5).

Keywords Detrital zircons · U/Pb dating · Hf isotopes · Of impurity trace-element content · Crimea · Dobrogea · Pontides · Paleogeographic reconstructions

Electronic supplementary material The online version of this article (https://doi.org/10.1007/s00531-019-01770-2) contains supplementary material, which is available to authorized users.

✉ N. B. Kuznetsov
kouznikbor@mail.ru

E. A. Belousova
elena.belousova@mq.edu.au

W. L. Griffin
bill.griffin@mq.edu.au

S. Y. O'Reilly
sue.oreilly@mq.edu.au

T. V. Romanyuk
t.romanyuk@mail.ru

S. V. Rud'ko
rudserega@yandex.ru

1 Geological Institute, Russian Academy of Science, Pyzhevsky Lane 7, Moscow 119017, Russia

2 ARC Centre of Excellence for Core to Crust Fluid Systems and GEMOC ARC National Key Centre, Department of Earth and Planetary Sciences, Faculty of Science and Engineering, Macquarie University, North Ryde, Sydney, NSW 2109, Australia

3 Gubkin Russian State University of Oil and Gas, Leninsky Pr 65, Moscow 119991, Russia

4 Schmidt Institute of Physics of the Earth, Russian Academy of Science, B. Gruzinskaya Str., 10, Moscow 123242, Russia

Introduction

The Balkans–Anatolia–Black Sea–Caucasus region (BABSC) is a segment of a gigantic Mesozoic–Cenozoic collision zone—the Alpine–Himalayan fold-thrust belt that formed as a result of convergence between the northern Arct-Laurasian and southern Gondwanan continental masses (Fig. 1a). Geological (geodynamic, stratigraphic, and geochronological data) and geophysical data have allowed reconstructions of the main stages of the Phanerozoic geodynamic evolution of this region (Stampfli and Borel 2002; Stampfli et al. 2002, 2013; Murphy et al. 2000, 2004a, b, c; Cavazza et al. 2004; Saintot et al. 2006; Murphy and Nance 2008; Schmid et al. 2008; Strachan et al. 2014; Samson et al. 2005; Stampfli et al. 2002, 2013; Stampfli and Kozur 2006; Okay et al. 2001, 2006, 2015, 2018; Linnemann et al. 2007, 2011, 2014; Nikishin et al. 2011; Natal'in et al. 2012; Nance et al. 2013; von Raumer et al. 2013, Gallhofer et al. 2015, 2016; Okay and Nikishin 2015; and references therein). According to these ideas, in the Early Neoproterozoic the Rodinia

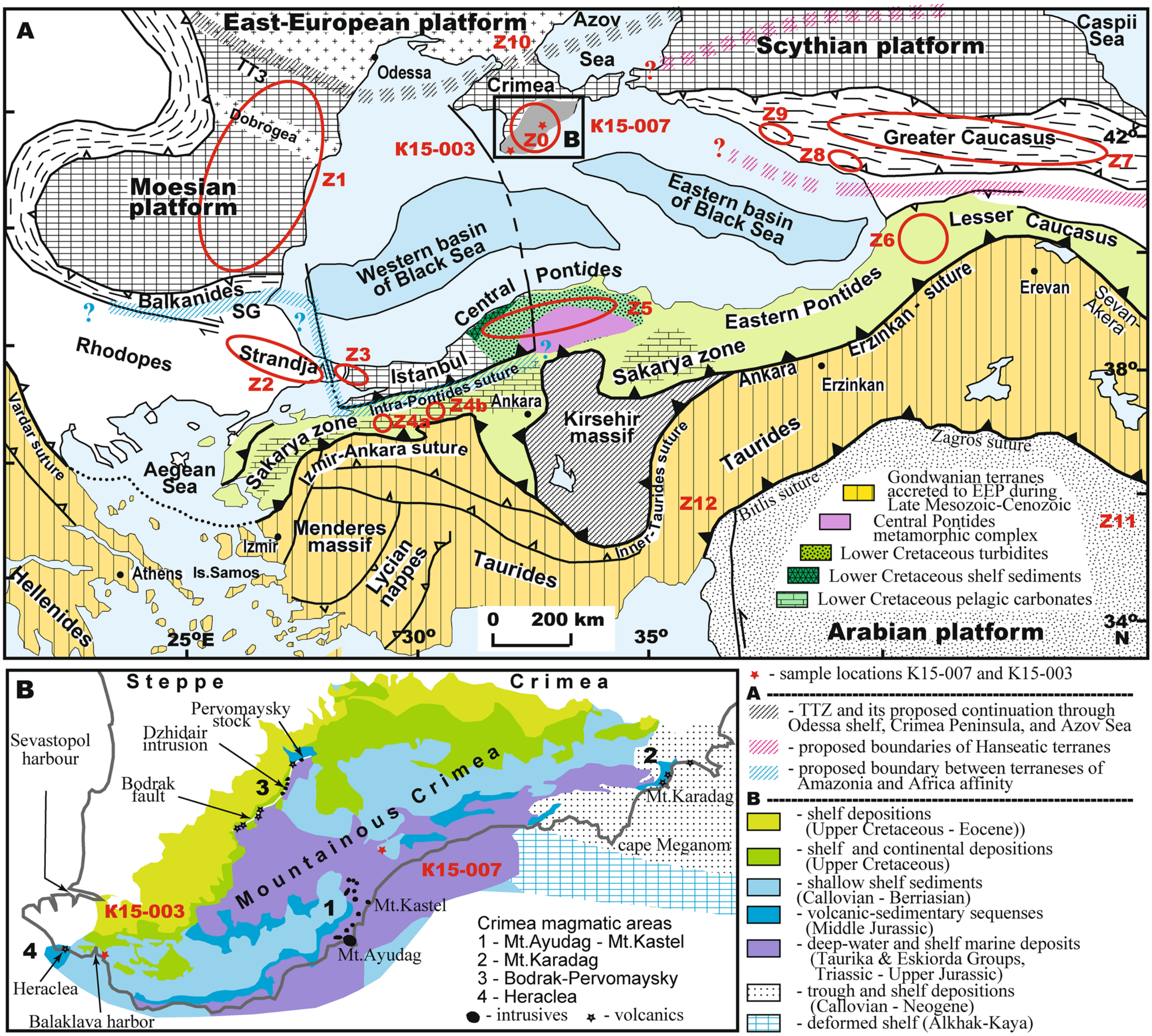

Fig. 1 **a** Main geological–tectonic structures of the Anatolia–Black Sea–Caucasus region after Okay et al. (2001) with simplifications and additions from Okay et al. (2013) and the Balkans–Moesian platform region after Gallhofer et al. (2015), as well as locations of sampling sites K15-007 and K15-003. TTZ, Teisseyre–Tornquist zone. Red ellipses and labels **Z0–Z12** mark regions discussed in text with data for detrital zircons from (meta)sedimentary rocks. **b** The geological setting of the Mountainous Crimea with magmatic areas after (Solov'ev and Rogov 2010; Nikishin et al. 2015a) with simplifications and additions by the authors

supercontinent had disintegrated with the complete isolation of the Baltica paleo-continent, which is the Precambrian foundation of the Eastern European Platform (EEP). Then, Baltica participated in the assembly of the northern continental masses in Arct-Laurasia, occupying the marginal southern position in this new expanding continent. In the Late Neoproterozoic and Paleozoic, the southern and southwestern margins of Arct-Laurasia were bounded by the Paleo-Tethys ocean, the lithosphere of which was subducted beneath the continent. Therefore, during Paleozoic time, the southern margin of Baltica (or the Baltic part of composite continents including Baltica) grew consistently by the accretion of terranes with different origins: they either were split off from Arct-Laurasia, or from various parts of Gondwana (Hanseatic and Cadomic–Avalonian terranes), or were initially formed as intra-oceanic formations—volcanic arcs, oceanic plateaus, and relics of ocean basins (Galatian terranes). As a result, towards the end of the Carboniferous (~ 300 Ma), the southern and southwestern margins of the Baltica had grown by a wide band of terranes (Fig. 2a). At the end of Permian and Triassic time, a large strip-like fragment of the continental lithosphere (Cimmerian terranes) had broken away from the northern periphery of Gondwana and begun to drift towards Baltica. This led to the closure of Paleo-Tethys and the opening of Neo-Tethys (Fig. 2b) in Triassic—Early Jurassic time. Relics indicative of the closure of this oceanic basin are considered to be the following suture zones (Fig. 1a): on the Anatolian Peninsula, Izmir–Ankara–Erzincan; in the Balkans, Vardar; in the Caucasus, Sevan–Akera. The Bitlis and Zagros sutures are Late Cenozoic zones marking the collision of the Arabian Plate with Northern Eurasia (Okay et al. 2010; Moghadam et al. 2012; Yılmaz et al. 2014; Chiu et al. 2013). Those parts of the Cimmerian terranes that were rifted from northeastern Africa, and possibly part of Arabia, are now the foundation of southern and eastern Turkey and are collectively called the Taurides (or Anatolides–Taurides).

Available geochronological data, including ages of ophiolites and high-pressure and ultra-high-pressure complexes, as well as stratigraphic correlations of radiolarians in ophiolites, constrain the lifetime of the Neo-Tethys ocean to an interval from 255 to 65 Ma (Goncuoglu et al. 2008, 2012; Galoyan et al. 2009; Rolland et al. 2009). The Intra-Pontides suture is a relic of the closure of the Izmir–Ankara ocean (or the Intra-Pontides ocean), which opened in the Early

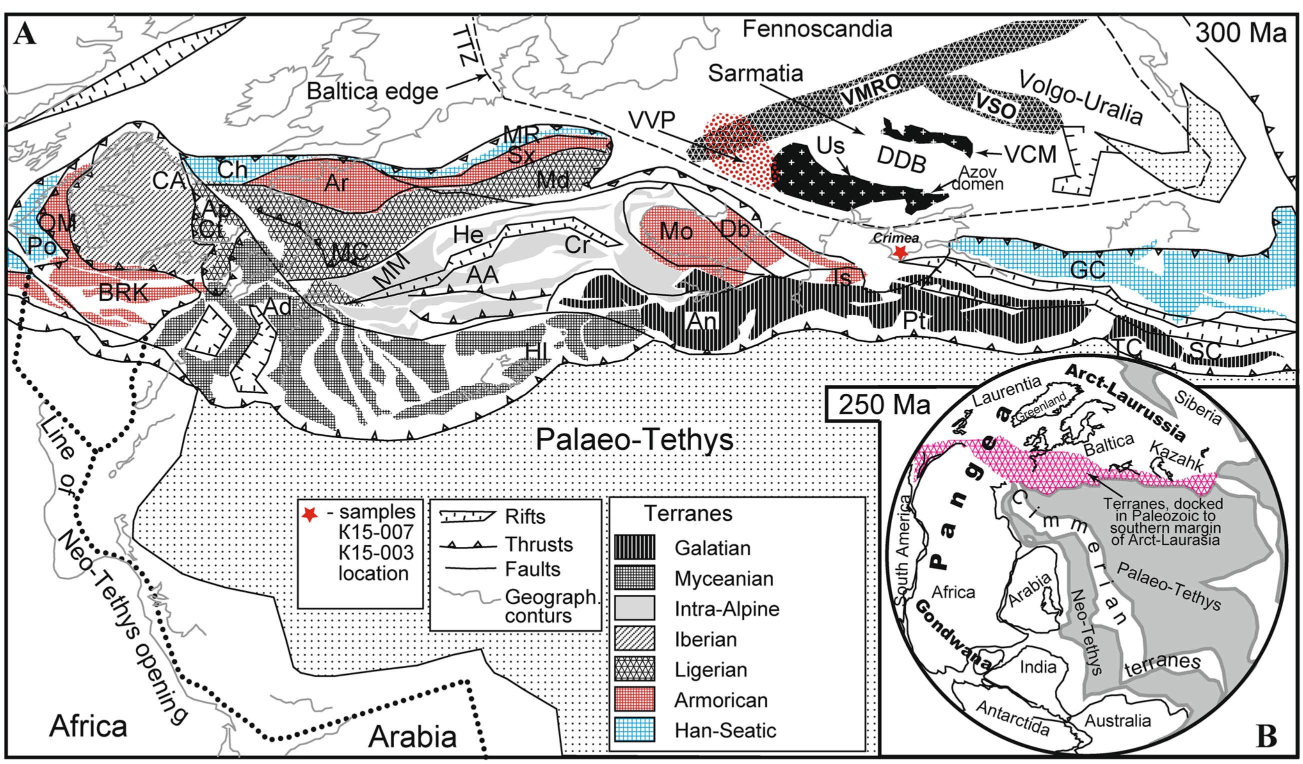

Fig. 2 Paleotectonic reconstruction for Balkans–Anatolia–Black Sea–Caucasus region at ~ 300 Ma **a** and ~ 250 Ma **b**, based on (Stampfli et al. 2013). Terranes docked to the southern margin of Arct-Laurussia: Pt—Pontides, GC—Greater Caucuses, Is—Istanbul-Zonguldak, Db—Dobrogea; Mo—Moesia. Baltica (Precambrian foundation of East European Platform) elements: Us—Ukrainian shield; VCM—Voronezh crystalline massif; DDB—Dnepr–Donetsk basin; VSO—Volgo-Sarmatian (Volgo-Don) Orogen; VMRO—Volyn-Middle-Russian Orogen; VVP—Volyn Volcanic province. TTZ—Teisseyre–Tornquist Zone

Triassic and closed, according to various estimates, from the Early Cretaceous to the Early Paleogene (Celik et al. 2011; Cavazza et al. 2012; Akbayram et al. 2013). The Pontides are Triassic–Cretaceous complexes formed inside and on the margins of the Izmir–Ankara ocean. Within the Pontides, there are three different areas (terranes): Strandja (basement of the Thrace basin); Istanbul–Zonguldak (or Istanbul); and Sakarya (Okay and Tüysüz 1999).

During the Late Cretaceous and Cenozoic, the BABSC was subjected to meridional stretching, accompanied by large-scale faulting, folding and eruptive deformation, as well as magmatism. As a result, the Black Sea marine basin (Late Cretaceous—Eocene) formed with oceanic crust in its deepest parts, known as the Western and Eastern basins (Hippolyte et al. 2010; Georgiev et al. 2012; Nikishin et al. 2015b, c). The Istanbul block was detached from the Dobrogea–Moesia block and moved to the southern margin of the Black Sea (Fig. 1a).

However, this comprehensive framework for the sequence of main events in BABSC is still not generally accepted; its stages and details of the evolution of individual regions are still controversial. Recent studies argue that the Paleozoic evolution of Tethys was much more complicated in space and time than a simple closure of Paleo-Tethys and the opening of Neo-Tethys due to the drift of the Cimmerian terranes (Ustaomer et al. 2016; Avigad et al. 2016). After and during accretion to the southern and southwestern margin of the Baltica, terranes underwent the Caledonian, Variscan, Cimmerian, and Alpean orogenies (Dokuz 2011; Kroner et al. 2008; Okay et al. 2015), as well as episodes of shearing and extension (Nikishin et al. 2015b, c), which obscured the ultimate origin of those terranes. Therefore, the primary nature of some crustal blocks of the BABSC, the time frames for the existence of individual volcanic arcs, the time of their docking to the continent, the direction and slope of subduction zones, the locations and times of shear activity, and formation of basins are still being refined (see, e.g., Linnemann et al. 2004; Natal'in et al. 2012; Meinhold et al. 2013; Topuz et al. 2013b). The exact position of the southern edge of the Precambrian foundation of the EEP (Baltica) within BABSC is also unclear. Usually, geophysical and indirect geological data trace it from the Teisseyre–Tornquist zone (TTZ) in Europe through the Odessa shelf, then along the neck of the Crimea Peninsula and the southern edge of the Azov Sea into the inner parts of the Scythian plate and further into the northern Pri-Caspii region (Stampfli et al. 2013).

An integrated isotopic–geochemical study of detrital zircons from sedimentary strata can help in solving the question on the nature of the crystalline basement of the Crimea, and provide more information on the paleogeographic depositional environment and provenance. A number of recent studies that applied this approach have been able to correlate the basement blocks of the various regions surrounding the Black Sea essentially to different parts of Gondwana (Henderson et al. 2016). The basements of the Greater Caucasus, the Lesser Caucasus, and most of Eastern Pontides have affinities to the Arabian–Nubian Shield and Iran (Ustaomer et al. 2013; Moghadam et al. 2012, 2017). The basement of Central and Western Pontides is related to northern and northeastern Africa (Meinhold et al. 2011; Avigad et al. 2016). The blocks forming part of the basement of the Moesian plate (Moesia), the Serbo-Macedonian massif, Northern and Central Dobrogea (see insert in Fig. 3b), and the Istanbul block are considered as a part of Amazonia (Bozkurt et al. 2008; Okay et al. 2008, 2011; Meinhold et al. 2010; Ustaomer et al. 2011; Balintoni and Balica 2016).

Since the regions surrounding the Crimea such as the Sarmatian part of the EEP (including the Ukrainian Shield), the Dobrogea, the Caucasus, and the Pontides are now characterized by sufficient geochronological data (dating of both crystalline complexes, and detrital zircons from strata of various ages) that the comparison of these data with similar geochronological information on the Crimea would make it possible to identify the similarities and differences in the different structural units of the Crimea and compare their provenance signals with those in the surrounding regions. However, geochronological data for the Crimea are still very scarce. This work aims to fill this gap, at least partly, by an integrated isotopic–geochemical study of detrital zircons from the Upper Jurassic conglomerates of the Mountainous Crimea (MtCr) (samples K15-007 and K15-003, Fig. 1).

Geological settings of the mountainous crimea

The geology of the MtCr has been well studied previously (Nikishin et al. 2015a and references therein). Paleozoic basement has been documented by drilling beneath Steppe Crimea and supposedly underlies Upper Triassic to Lower Jurassic sequences of the Crimean Mountains. However, the question of the origin of the crystalline basement of the Mountainous Crimea has not been solved, since there are no geological outcrops or drill holes that have reached it. In the paleotectonic reconstructions, Crimea falls into the conjugation of terranes of different types. On one hand, the geological correlations of the Mesozoic sedimentary complexes of MtCr give grounds to correlate the MtCr with the coeval strata of the Pontides. During the Mesozoic, before the opening of the Black Sea depression, the complexes of the MtCr and the Pontides were located near one another and underwent similar geological evolution (Okay and Nikishin 2015). This provides indirect evidence that the basement of the Crimea is similar to the Pontides basement. At the same time, deep seismic studies indicate that the structures of the Dobrogea basement can be traced from the west through

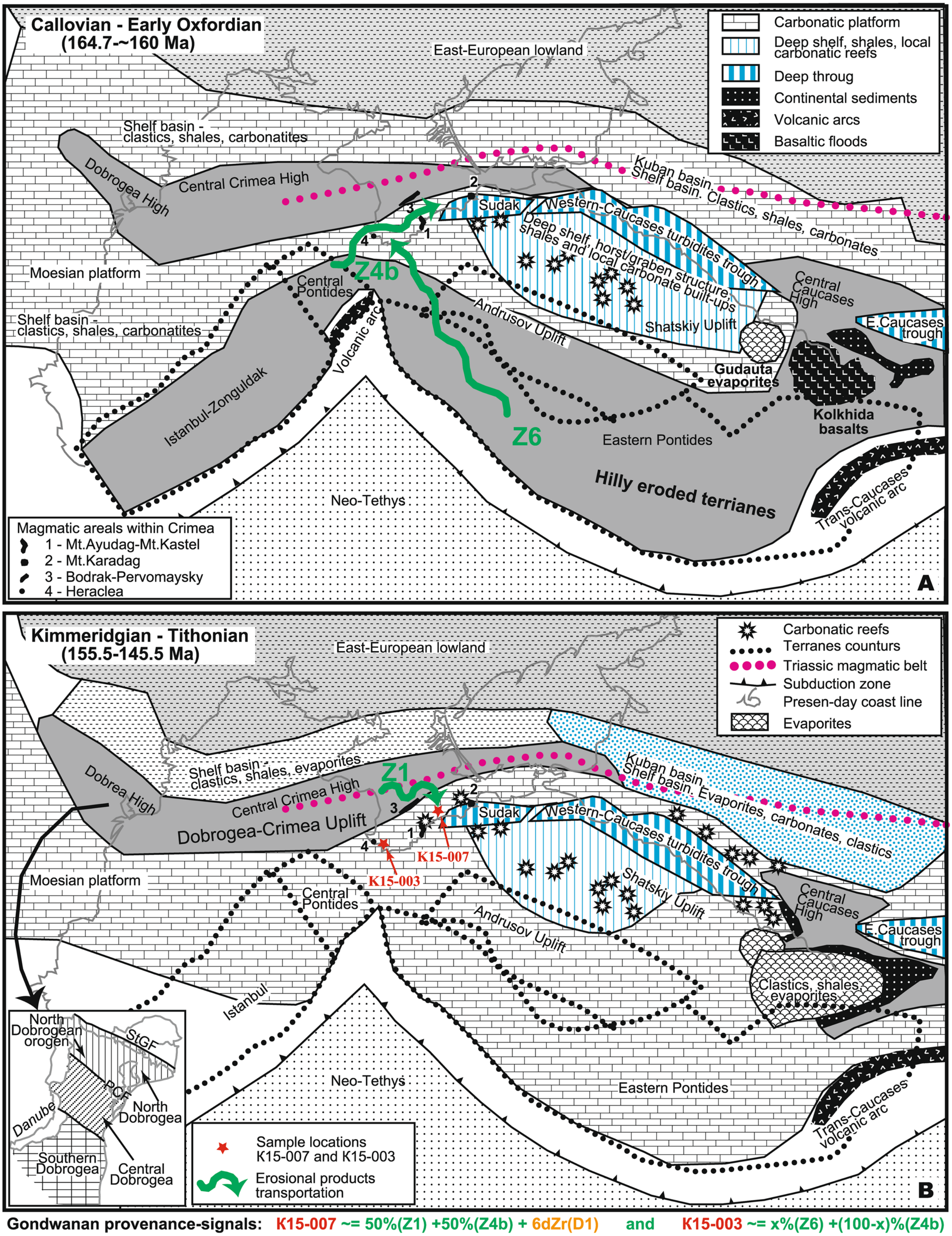

Fig. 3 Paleogeographic reconstruction for the Callovian–Early Oxfordian **a** and Cimmeridgian–Tithonian **b** for the Crimea and adjacent areas after Nikishin et al. (2015a). Insert in **b**: a tectonic scheme of present-day Dobrogea after Seghedi (2012)

the Odessa shelf to the MtCr (Starostenko et al. 2015), and the structures of the Indolo-Kuban trough of the Cis-Caucasia—to the Steppe Crimea from the east (Adamia et al. 2011). Thus, indirect information allows us to consider that the basement of the Crimea is related to the basements of both the Central/Western Pontides, or the Dobrogea, or the Greater Caucasus.

In the Middle and Late Jurassic, the Neo-Tethys Ocean was closing and its lithosphere was subducting under the southern edge of Arct-Laurasia. The position of the trench is reconstructed along the southern edge of the Istanbul, Central, and Eastern Pontides blocks of (Fig. 3a). The end of the Jurassic is important in the geological evolution of the BABSC, as it marked a change from the near-meridional compression that accompanied the closure of the Neo-Tethys ocean to the near-meridional extension that led to the formation of the Black Sea basin.

In Callovian–Early Oxford time (Fig. 3a)—the stage immediately preceding the time of accumulation of the Upper Jurassic conglomerates—the Istanbul block and the Central and Eastern Pontides blocks still were uplifted and being extensively eroded. In Kimmeridgian–Tithonian time (Fig. 3b), during the accumulation of the Upper Jurassic conglomerates, the Istanbul, Central, and Eastern Pontides blocks began to subside and the crust began to extend, forming the future Black Sea basin. At the time of the formation of the Upper Jurassic conglomerates, the Istanbul, Central and the most western Eastern Pontides blocks were below sea level and a carbonate platform began to develop on the former uplifts (Masse et al. 2009). Thus, the transport of detritus from Pontides to the shelf of the Dobrogea–Crimea Uplift from the southern side became impossible, but on the contrary, the transport of the erosional products of the Dobrogea–Crimea Uplift would have been intensified. If the complexes of the Pre-Mesozoic foundation of the Crimea within Dobrogea–Crimea Uplift were exhumed to the erosional level at that time, then their erosional products could contribute into the Upper Jurassic conglomerates. Thus, the provenance signal of the Pre-Mesozoic Crimea had a chance to survive in the Upper Jurassic conglomerates.

Sample collection

The conglomerates of Mt. Southern Demerdzhi are accepted as a stratotype of the Upper Jurassic Demerdzhi Formation due to their availability, good exposure, and access to the outcrop. At the present time, two strata (upper and lower) are distinguished within the Demerdzhi Fm., which are separated by angular unconformity. Sample K15-007 was collected from a lens of light gray sandstone situated at the base of the section of the upper stratum of the conglomerates on the western slope of Mt. Southern Demerdzhi (44°44′41.9″S; 34°24′28.4″E). Sample K15-003 was collected from the lens of light gray gravel sandstone located at the base of the rock escarpment on the southeastern slope of Mt. Sepia of Balaklava harbor (44°29′31.09″S; 33°37′16.69″E).

Analytical methods

The study was carried out using the TerraneChron®, analytical approach (Griffin et al. 2000, 2002, 2004, 2006, 2007; Belousova et al. 2002, 2006) developed at the CCSF/GEMOC Center (Macquarie University, Sydney). The methodology integrates in situ U/Pb age, trace element, and Lu/Hf-isotope analyses on zircons. Such an integrated approach makes it more reliably to identify the source rocks of detrital zircons and to reconstruct the evolution of the supplying provinces than can be done based on U/Pb ages of detrital zircons only (Peytcheva et al. 2008). The analytical work on detrital zircons was carried out using the LA–ICPMS and LA–MC–ICPMS techniques. The CART classification (Belousova et al. 2002) was used for the classification of zircons in terms of the composition of their parental magma. The granitoid rocks in this classification are subdivided according to their silica content into three groups: low-SiO_2 (< 65%), intermediate (SiO_2 = 65–75%), and high (SiO_2 > 75%). For the sake of briefness, these groups are called, respectively, «diorite», «granite» and «leucogranite» and corresponding zircons as «dioritic», «granitic», «leucogranitic», etc. Initial analytical data are provided in ESM A. Descriptions of measurement parameters, methodologies, and constants used to process primary analytical data are reported in the previous studies and in ESM B (Figs. B1–B8).

Analytical results

U–Pb age results

Sample K15-007. A total of 95 analyses were carried out for this sample (Fig. B1). For 7 grains, strongly discordant age values ($|D| > 10\%$) were obtained and one measurement (№10) showed a very large analytical error − 2835 ± 155 Ma. Those were rejected from further considerations. The remaining 87 analyses were used to plot the histogram and probability density curve (*PDC*) (Fig. B2a). The five youngest ages on the concordia diagram form a separate compact cluster **S** with a concordia age of 153.91 ± 1.56 Ma (Fig. B1d, B2b).

The zircons were subdivided according to their age pattern into 10 groups, referred as **D1–D10**. The most representative—groups **D2** and **D3** (each is over a quarter of all zircons) comprise zircons with Permian–Triassic ages. The zircons of cluster **S** together with another zircon of №147 of similar age 164 ± 2 Ma (D = 7%) form a group **D1**. Archean and (Late- + Middle-) Paleoproterozoic zircons form distinct groups **D10** and **D9**, respectively. Zircons with overlapping ages are combined into compact groups **D4**, **D5**, **D6,** and **D7**, the remaining zircons (whose ages are scattered in the interval 810–1550 Ma) are assigned to group **D8**. The age interval of 2.15–2.55 Ga is not represented by any grain.

Sample K15-003. A total of 70 analyses were performed for this sample. For 3 grains, strongly discordant analyses (│D│ > 10%) have been obtained (Fig. B3a). The remaining 67 values were used to plot the age histogram and *PDC* (Fig. B4a). The zircons were divided into 9 groups according to their age distribution and designated as **B1**–**B9**. Zircons younger than 500 Ma form the groups **B1**–**B4**, and Cambrian–Neoproterozoic zircons–groups **B5**, **B6,** and **B7**. Archean and (Late- + Middle −) Paleoproterozoic zircons form the groups **B9** and **B8**, respectively, separated by an age gap between 2.15 and 2.35 Ga, in no grains are recorded. The Mesoproterozoic age interval (1050–1700 Ma) is represented only by grain №59 with a near-concordant age of 1444 ± 42 Ma (*D* = 3.9%). It shows no common-lead contamination, and a normal trace-element content (e.g., P is 1049 ppm, Th/U = 1.15). The poorly developed zoning in the CL image (see the insert in Fig. B3) may suggest a non-magmatic origin of this zircon.

Trace-element content and classification of zircons by their parental rock types

The Th/U ratio commonly is used to distinguish zircons of metamorphic (Th/U < 0.1) and igneous (Th/U > 0.1) origin (Teipel et al. 2004).

In sample K15-007, only one zircon (№2) showed a Th/U ratio of less than 0.1 (Fig. B2b) and is classified as «metamorphic»; this is consistent with the absence of clear oscillatory zoning in its CL image (the insert in Fig. B2a).

In sample K15-003, two zircons showed distinctly low Th/U ratios: №20 = 0.086 and №71 = 0.003 (Fig. B4b) and were classified as «metamorphic». The CL image of zircon №20 (the insert in Fig. B4b) is convincingly «metamorphic»—without any zoning, but the CL image for №71 (the insert in Fig. B4a) displays a complex structure: an inherited core with oscillatory zoning and relicts of older zircon blocks in the center and a thin light-CL rim suggesting a metamorphic overgrowth.

CART classification The CART algorithm (Belousova et al. 2002) was not applied to grains of metamorphic origin (Fig. B5). Application of the CART classification to the rest of the grains indicates that the parent rocks of the vast majority of zircons in both samples were most likely «granites» and «diorites». Although the subdivision of granitoid rock sources of zircons into «diorites» and «granites» is based on their Yb content, zircons of these types could be also statistically well subdivided according to the total REE (separation value of ~ 1200 ppm) (Fig. B6) and Y contents (Y border value of ~ 1500 ppm) (Figs. B6a and B8a). The samples differ significantly in the proportions of «granitic» and «dioritic» zircons: in the sample K15-007 they are approximately equally divided (39 and 35), and in sample K15-003 «granitic» zircons are almost twice as abundant as «dioritic» ones (38 vs 22). The most interesting result of the CART classification is the detection of zircons, the sources of which were most likely specific or «exotic» rocks such as «carbonatite», «syenite/monzonite» and «leucogranite». The three «carbonatitic» (№37, 51 and 123) and four «syenites-monzonites» (№73, 93, 112, and 144) zircons in the sample K15-007 have similar ages and were designated as clusters **C** and **S,** respectively.

Lu–Hf-isotope analysis of the detrital zircons

Sample K15-007 The Lu–Hf-isotope composition was studied for 89 grains (Fig. 4a). For 3 zircons (№41, 49 and 71), a strongly variable signal was recorded during the ablation, indicating a significant isotopic heterogeneity of the analyzed material. The remaining 86 analyses produced stable signals and homogeneous results. Zircons from this sample recorded a spread of ε_{Hf} values from about +13 (№4) to − 20 (№83). Estimates of the crustal model age T_{DM}^{C} range from 0.58 (№44) to 3.44 (№6) Ga.

The three Middle Neoproterozoic zircons forming the **D7** group have significantly negative ε_{Hf} values, including grain №83 with the lowest ε_{Hf} of − 20.0 ± 0.95, indicating the involvement of the Archean crust (T_{DM}^{C}, is about 2.7 Ga). Such a cardinal difference between these zircons from the near-coeval zircons of groups **D8** and **D6** is an additional argument for isolating these three zircons into a separate **D7** group, despite its statistical non-representativeness.

The group **D1** of the youngest zircons is the most interesting. It consists of 6 zircons: «dioritic» zircon №147 (164 Ma) and five zircons of cluster **S** with ages about 154 Ma. Cluster **S** includes four zircons (№ 73, 93, 112 and 114) that are classified as «syenite/monzonitic», and one as «dioritic» (№ 62). Both «dioritic» and «syenite/monzonitic» zircons show negative ε_{Hf} ranging from − 1.5 to − 6.9 and T_{DM}^{C} of 1.16–1.54 Ga suggest all zircons of cluster **S** originated from a single local source. The Hf-isotope composition of zircon №147 with ε_{Hf} = 2.5 ± 0.9, T_{DM}^{C} = 1.05 Ga is quite different from those of the zircons from cluster **S**, indicating derivation from another source. In summary, the zircons of cluster **S** were generated during an igneous event around 154 Ma ago; their parental magmas were alkaline in composition and derived from a protolith not younger than Mesoproterozoic (T_{DM}^{C} = 1.16–1.54 Ga).

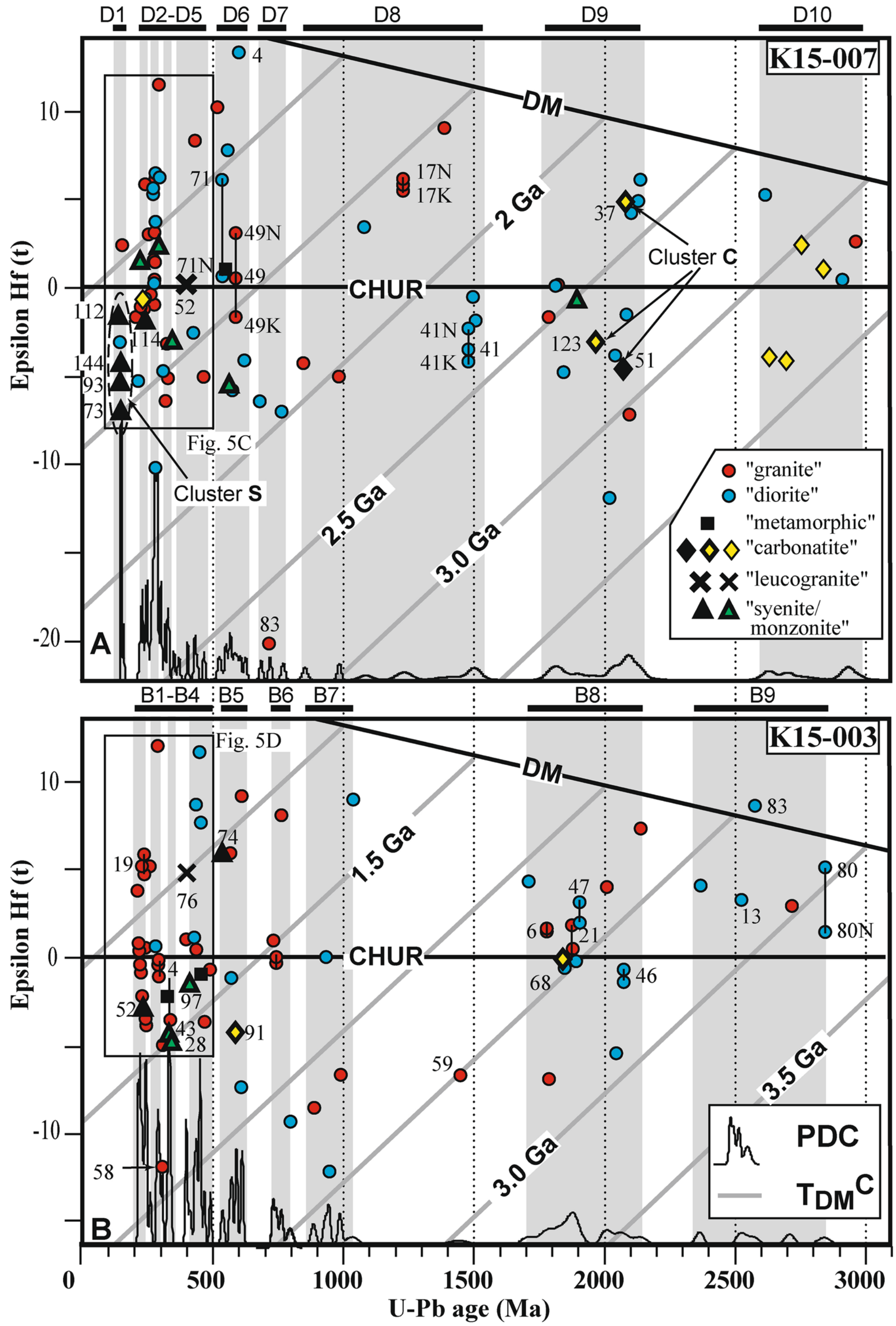

Fig. 4 Diagram of ε_{Hf} vs U–Pb age for samples K15-007 **a** and K15-003 **b**. The vertical lines show variations recorded within a single analysis. Black bars on the top and gray background show the time intervals of the groups of zircons **B1**–**B9** and **D1**–**D10** as discussed in the text. *PDC* is a probability density curve, T_{DM}^{C} is the Hf crustal model age of the protolith

Sample K15-003. The Lu–Hf-isotope analyses were done on 67 grains from this sample (Fig. 4b). In zircons №80, 47 and 21, rather significant variations of Hf-isotopic composition were recorded during the analysis, and these data are not considered further. The remaining ε_{Hf} values for this sample range from +12 (№2) to − 12 (№55). Estimates of crustal model ages T_{DM}^{C} range from 0.52 (№22) to 3.16 (№80) Ga.

Discussion

In this section, first, the results from samples K15-007 and K15-003 are compared, and geodynamic constraints on their possible primary sources are outlined. Then, possible sources are analyzed considering that the zircon can be derived either directly crystalline complexes [primary sources, see schemes of locations within **BABSC** the crystalline complexes with Jurassic, Triassic, Permian–Carboniferous, as well as Late Neoproterozoic–Cambrian and Ordovician–Devonian ages in ESM C (Figs. C1–C4)] or (meta)sedimentary complexes (secondary sources).

To constrain possible secondary sources, the characteristics of detrital zircons from samples K15-007 and K15-003 are compared with published data available on the pre-Upper Jurassic deposits of neighboring regions (their locations are denoted **Z1–Z4**, **Z6–Z8,** and **Z10–Z12** in Fig. 1), and data for Lower Cretaceous and younger sediments of neighboring regions (their locations are denoted by **Z0**, **Z5,** and **Z9** in Fig. 1) are explored. The latter could not be a source of zircons for the Upper Jurassic conglomerates, since they are younger, but the comparison is useful, because it provides additional paleogeographic information.

Comparison of the results of studied detrital zircons and constraints on the geodynamic nature of their primary sources

In general, the detrital zircons from both samples studied here (Figs. 4, 5) show many similarities, but also some significant differences. One major dissimilarity is the significantly different proportions of the «granitic» and «dioritic» zircons: in sample K15-007, where they are approximately equal (43% and 41%), but in sample K15-003 «granitic» zircons are almost twice as abundant as «dioritic» ones (39% vs 23%). At the same time, majority of «granitic» grains are younger than 500 Ma in both samples.

Zircons in both samples were divided into groups labeled **D1**–**D10** for sample K15-007 and **B1**–**B9** for sample K15-003. The U–Pb age distribution patterns of zircons from both samples show similarity in the broad time intervals from the Jurassic to the Archaean and in the general characteristics of the age spectra, including major Triassic and Permian populations with a good match of age peaks on the *PDC*, and minor populations of the Carboniferous age and older with comparable individual age peaks.

However, there are quite significant differences in some age groups, especially Archean zircons of groups **B9** and **D10**. In the **D10** group, all ages are older than 2.9 Ga, while in the group, **B9** zircons with ages of 2.35–2.6 Ga are found, together with zircons older than 2.9 Ga. The Hf-isotope composition also records a small but certain difference. In the **B9** group, the Hf isotopes have more juvenile composition ($\varepsilon_{Hf} > 3$, and for № 83—even comparable to DM), than in the **D10** group, where zircons have mostly weakly positive ε_{Hf}, and for two zircons, ε_{Hf} is as low as − 3. Since no zircons were found that would show the presence of the oldest Palaeo-Archaean material in the magma sources, the most probable sources of Archean zircons from both samples are intra-oceanic arcs and arcs started on rifted crust that was not older than Mesoarchaean. At the same time, the significant differences in U–Pb

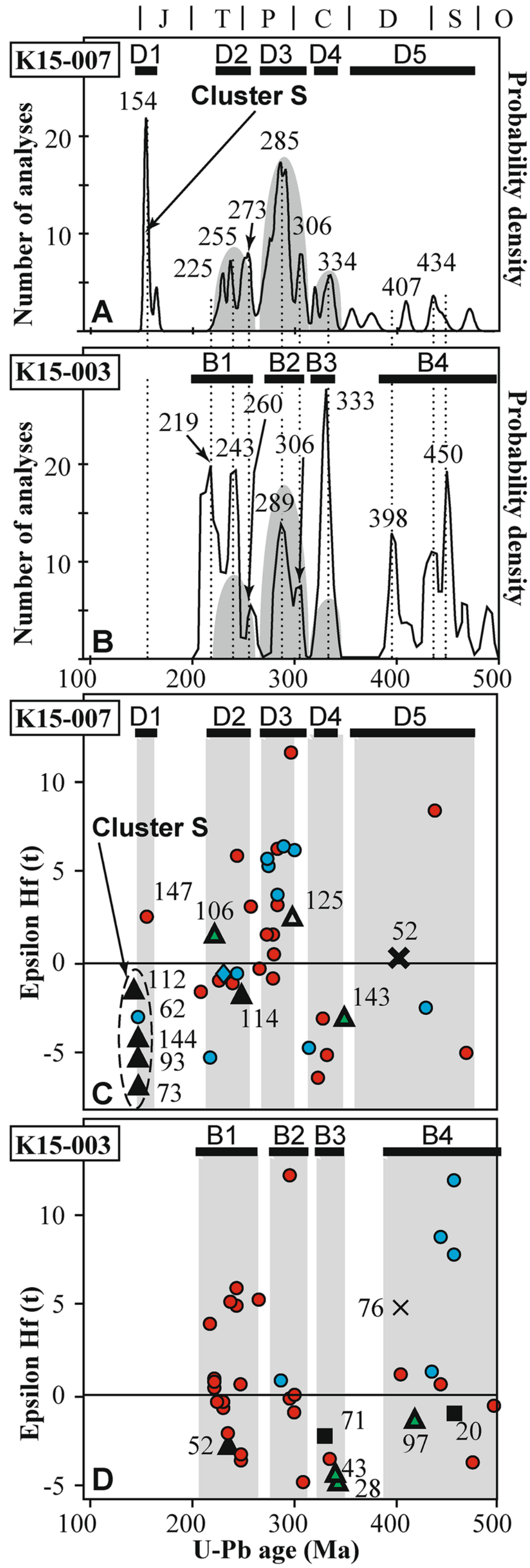

Fig. 5 Comparison of age groups (**a**, **b**) vs ε_{Hf} (**b**, **d**) for detrital zircons from samples K15-007 and K15-003 for ages less than 500 Ma. Black bars and inscriptions **B1–B4** and **D1–D5** show the time intervals of the identified groups in the samples. Gray semi-ellipses on A and B mark groups showing good age resemblance

age, Hf-isotope, and trace-element composition do not allow us to assume a common source(s) for the Archean zircons from samples K15-003 and K15-007.

The cardinal differences between the samples are in the 850–1500 Ma age interval. In the sample K15-003, only one zircon №59 of Mesoproterozoic age was found, while in the K15-007 sample, there were 7 zircons with the ages evenly distributed along the Mesoproterozoic time interval, with no peaks on the *DPC*. There are only 2 zircons of Early Neoproterozoic age in sample K15-007, and 5 in the sample K15-003 (**B7**). Parental rocks for all these zircons were distributed in evenly between «granites» and «diorites», so specific source rock types were not identified.

The compact groups of data points for zircons from groups **D4** and **B3** (Carboniferous) are very uniform in U–Pb age (with peaks at 334 and 333 Ma) and show only negative ε_{Hf} (− 2 to − 6), which indicates at least a Mesoproterozoic (~ 1.3–1.5 Ga) age for the protolith. Such zircons are likely to have an intra-plate origin, and originated from a single geographically restricted source.

The groups **D3** and **B2** have slightly different ages within Permian interval, with the peaks at 306 Ma, and 289–285 Ma being very well matched. One zircon in the **B2** group has slightly negative ε_{Hf}, while all the other zircons in both groups have moderately juvenile (mostly positive and near-zero ε_{Hf}) Hf-isotope signatures.

Triassic–Permian zircons from groups **D2** and **B1** show slightly different age intervals and *PDC* peaks at 225, 255, 273 Ma and 219, 243, 260 Ma, respectively, so that group **B1** seems to be «shifted» by about 10 Ma relative to group **D2**. In both groups, the «granitic» zircons dominate and show similar Hf-isotope signatures.

The zircons of the well-defined groups **D2**, **D3,** and **D4** in sample K15-007 and **B1**, **B2,** and **B3** in sample K15-003 record episodes of magmatic activity in the **BABSC**, indicating that the products of destruction of the crystalline complexes contributing to both samples. A significant part of the zircons from groups **D2**, **D3**, **B1,** and **B2** is definitely of a local regional origin and was generated in the suprasubduction structures or intra-oceanic arcs of the Neo-Tethys. At the same time, the Hf-isotope results do not record any significant contribution of crustal material that is older than Mesoproterozoic.

In the K15-003 sample, no zircons corresponding to zircons from group **D1** were found. This is an additional argument that the source of group **D1** zircons was situated near the K15-007 sampling site.

Late Jurassic rocks of Crimea and Pontides as potential primary sources of zircons for cluster S of sample K15-007

Magmatic complexes of Jurassic age are widely distributed in the eastern part of **BABSC** (Fig. C1). Complexes with Middle–Early Jurassic ages are very widespread in the Crimea, Central and Eastern Pontides and in the Greater Caucasus. The Upper Jurassic complexes are less widely represented, but nevertheless magmatic and metamorphic complexes with Late Jurassic age are known in the Sredna Gora and Central-Eastern Pontides.

Four areas with outcrops of magmatic rocks are known within **MtCr** (Fig. 1b). Previous dating of magmatism in the **MtCr,** mainly based on stratigraphic and field observations/relationships, described all of these magmatic rocks as Jurassic or Cretaceous. However, new geochronological data have appeared in recent years, and a summary of the available results is presented in Fig. C2.

Late Jurassic magmatism, including an event at ca 154 Ma, is known both within the present-day **MtCr**, and in the Pontides. Several magmatic areas in the Pontides (Chamlikaya granites, meta-dacites of the Changaldag complex, metamorphites of the Kunduz complex and possibly others) and in the **MtCr** (Mt. Karadag area) with similar time intervals of magmatism might be considered as potential sources for zircons of cluster **S**. However, available data still do not allow us to identify the local source for zircons of cluster **S** from sample K15-007.

Potential primary sources of Archean and Paleoproterozoic zircons

The most logical primary source for the Archean and Paleoproterozoic zircons from samples K15-007 and K15-003 is the basement crystalline complexes of the ancient crustal blocks presently closest to the Crimea– Sarmatian part of EEP, including the Ukrainian Shield (Us), Voronegh Crystalline Massive (VCM) and the adjacent territories. Archean ages have been found for crystalline rocks of the VCM and Us basements, including the Podolsky and Azov domains (the latter is located close to the Crimea, see Fig. 2) with crystallization ages up to 3.7 Ga and model ages up to 3.9 Ga. Within the Sarmatian and adjacent parts of the EEP, the Paleoproterozoic complexes of accretionary collisional origin are known (Fig. 6a). A summary of the ages and references for these formations are given in ESM C (Fig. C5).

Recent studies of detrital zircons from Neoproterozoic meta-sedimentary rocks of the Ukrainian Shield (Shumlyanskyy et al. 2015), allow a comparison the studied zircons of the Crimea and the Us (**Z10**) (Fig. 6b). The most significant differences between the data sets are as following:

- No zircons with ages over 3 Ga have been found either in sample K15-007, or K15-003, while in the Us such zircons are common, together with ages over 3.5 Ga that otherwise are very rare around the world.

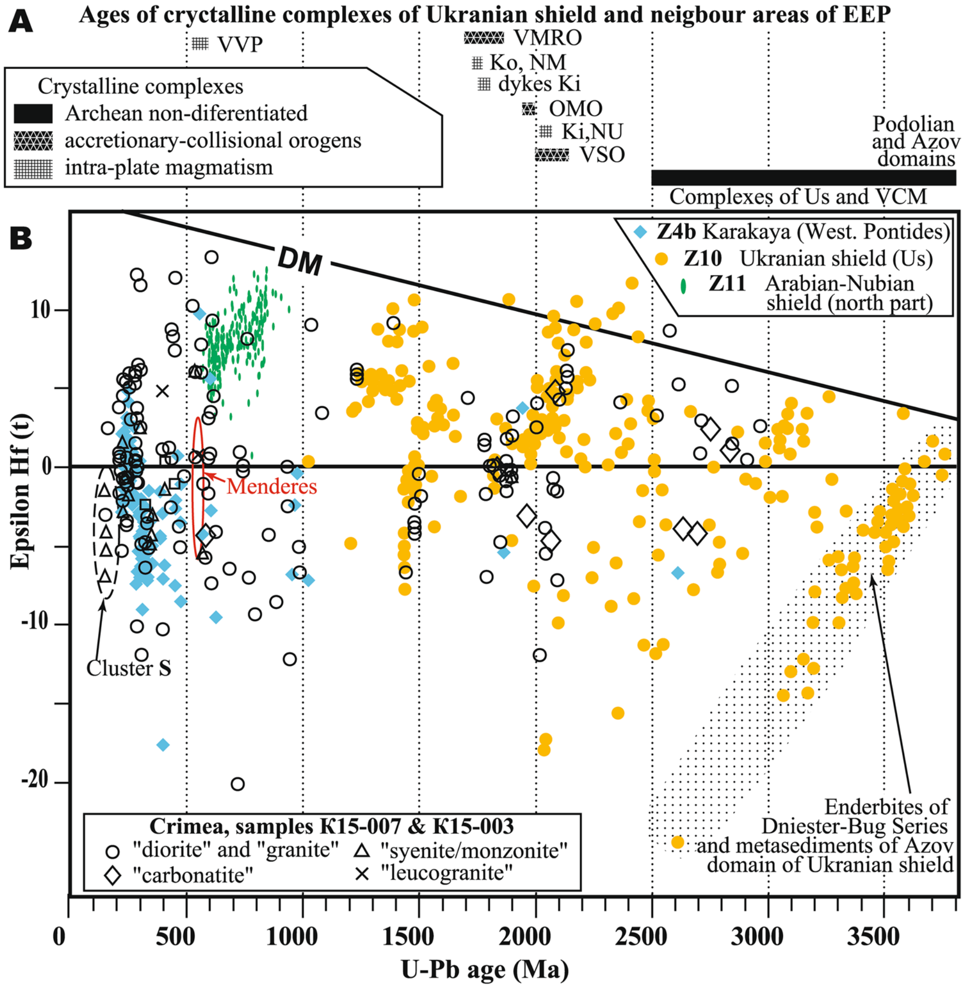

Fig. 6 Comparison of the results of U–Pb and Lu–Hf isotope study of detrital zircons from samples K15-007 and K15-003 with analogous data from neighboring regions of the **BABSC**. **a** U–Pb age data of some crystalline complexes of the Ukrainian shield and adjacent terrains (see refers in ESM C). Us—Ukrainian Shield, VCM—Voronezh crystalline massif, VSO—Volgo-Sarmatian orogen, VVP—Volyn volcanic province, OMO—accretionary orogen Osnitsk -Mikashevichi (2.0–1.95 Ga), VMRO—Volyn-Middle-Russian orogen (1.8–1.75 Ga). Plutons: Ki-Kirovograd (2.06–2.03 Ga), NU-Novoukrainskiy (2.04–2.03 Ga), KN-Korsun-Novomirgorodsky (1.76–1.74 Ga), Ko-Korosten, 1.74–1.8. Dykes in the Kirovograd massif—(1.81–1.77 Ga). **b** Comparison of the results of U–Pb and Lu–Hf isotope study for detrital zircons from samples K15-007 and K15-003 with analogical information on the detrital zircons from the Neoproterozoic meta-sedimentary rocks of the Us (**Z10**) (Shumlyanskyy et al. 2015) and the Karakaya complex of Western Pontides (**Z4b**) (Ustaomer et al. 2016), as well as the crystalline complexes of the Menderes massif (red oval, Avigad et al. 2016) and the northern part of the Arabian–Nubian shield (**Z11**) (Morag et al. 2011)

- The 2.15–2.6 Ga age interval is not represented in either of the studied samples, while zircons of such ages are widely distributed in meta-sedimentary rocks of the Us.
- No Archean zircons with significantly negative ε_{Hf} have been identified in samples K15-007 or K15-003. The minimum value found during this work is about − 2, while the ε_{Hf} values are as low as − 15 for Archean zircons of Us (Fig. 6b), thus corresponding to T^{C}_{DM} model ages older than 3.8 Ga, which are very rare around the world.

Such significant differences in the zircon characteristics suggest that there is a low probability of detrital products supplied either directly from the Us crystalline basement or from the ancient (meta)sedimentary strata of the Us to the studied Upper Jurassic conglomerates of **MtCr**.

Potential primary sources of Mesoproterozoic and (Early + Middle) Neoproterozoic zircons

Potential primary sources of the Mesoproterozoic and (Early + Middle) Neoproterozoic zircons could be crystalline complexes of ancient platforms or crystalline complexes of the basement of terranes docked to the Baltica in Mesozoic (Cimmerian terranes) and in Paleozoic.

In the Sarmatian part of the EEP, which is adjacent to the Crimea, no large-volume crystalline complexes with Mesoproterozoic and (Early + Middle) Neoproterozoic ages are known. Potential primary sources for such zircons transported from the EEP could only be complexes in its very remote parts such as the Sveco-Finnish and the Sveco-Norwegian regions of the Baltic Shield (Bogdanova et al. 2008). However, their considerable remoteness and the separation of the Crimea from the EEP by a sea strait at the time of formation of the Upper Jurassic conglomerates means that their detritus could contribute to the Late Jurassic conglomerates only through the recycling process.

Another potential primary source of (Early + Middle) Neoproterozoic zircons could be the Arabian–Nubian shield (ANS), which is a collage of Neoproterozoic island arcs that originated in the Mozambique ocean. In Cryogenian time, they were packed together and then in the Ediacaran were accreted to the Saharan metacraton (Avigad et al. 2016 and references therein). However, the available geochronological data indicate that the zircons from the northern part of the ANS (**Z11**) have exclusively juvenile origin with substantially positive ε_{Hf}, while zircons from our samples show predominantly negative ε_{Hf} (Fig. 6b). It is impossible to exclude the origin of some Neoproterozoic zircons from the ANS by recycling into the Upper Jurassic conglomerates, but the ANS zircons do not show the spectrum of ε_{Hf} values recorded in the (Early + Middle) Neoproterozoic zircons of samples K15-003 and K15-007.

Potential primary sources of Late Neoproterozoic, Paleozoic and Triassic zircons

Late Neoproterozoic and Cambrian–Devonian complexes (potential sources for groups D6–D5 and B5–B4) are widely distributed in the **BABSC** (Fig. C3). Complexes with ages of ~ 550–570 Ma are represented in the Sarmatian part of the EEP, including the Volyn volcanic intra-plate province (Fig. 2a). Large-scale rock complexes with Late Neoproterozoic and Early Cambrian ages are known in the Brunovistulian Domain, the Strandja massif, the Menderes massif, Puturge array, the basement of Istanbul, the basement of the Sakarya, the Dzirulla massif in the Caucasus, the Bitlis massifin western Turkey, the Sandikli region, and others. Ordovician–Devonian ages are much less common. Devonian magmatism is known in the Pontides (Sakarya zone, 401–396 Ma granite stocks). Ordovician-age metagranites are described from the Taurides, northwestern Turkey (discordant U–Pb ages of 330 ± 9 Ma for the Nelly granites, and 320 ± 19 Ma for the Camlikaya pluton).

Permian–Carboniferous complexes (potential sources for groups D4–D3 and B3–B2) Complexes with Permian–Carboniferous ages are widespread in the Balkans, Dobrogea, Greater Caucasus, Eastern Pontides and Western Pontides Fig. C4). Data available for the Derinoba and Kayadibi granites from the Eastern Pontides provide with the best fit for the characteristics of zircons in the **D4-B3** groups. They have yielded zircons with U–Pb ages of 304–317 Ma, and whole-rock Nd model ages of 1.5–2.15 Ga.

Triassic complexes (potential sources for groups D2 and B1) Triassic granite complexes are not known neither in the Pontides nor in the Caucasus (Fig. C5). However, traces of Triassic magmatic activity are known in the Steppe Crimea, where quartz dolerites and quartz diorites of 210 Ma age are known near the village of Severny. Triassic volcanism is also known in the Eastern Cis-Caucasia. In the Pontides, a Triassic magmatic province was defined by Genc (2004). According to petrological evidence, Triassic seamounts and oceanic islands have been recognised in Paleo-Tethys (Sayit et al. 2010; Okay et al. 2015). Based on the geophysical and indirect geological data, a Triassic magmatic belt is implied in the northern part of the Crimea (see review in (Okay and Nikishin 2015)), which is interpreted as the most significant source of the Triassic-age zircons in **BABSC**.

Secondary sources of zircons from neighboring regions

Dobrogea (Z1) The most complete summary of geochronological results for detrital zircons from the Dobrogea sandstones (26 samples, $n = 1833$) is presented by Balintoni and Balica (2016) (Fig. 7a). The summary contains data on rocks of Late Neoproterozoic–Late Paleozoic age. Considering this, the comparison of the data is useful only for ages > 300 Ma. This comparison shows a poor correspondence between Dobrogea and sample K15-003, but a very good resemblance between Dobrogea and sample K15-007 for ages > 400 Ma. The most striking coincidences of the age distribution are following:

- a very similar *PDC* in the Mesoproterozoic—Archaean time interval, with correlation of all age peaks;
- no older Mesoarchaean zircons in both sets;
- a lack of zircons (Crimea) and «clear minimum of *PDC*» (Dobrogea) in the interval 2.15–2.55 Ga,
- approximate correspondence of 600 Ma (Dobrogea) and 571 Ma (Crimea) age populations,
- good alignment of the 340 Ma (Dobrogea) and 334 Ma (Crimea) age peaks.

This similarity of the *PDC* is a strong argument that the sandstones of the Demerdzhi Formation contributed to the source of the K15-007 sample during the erosion of the

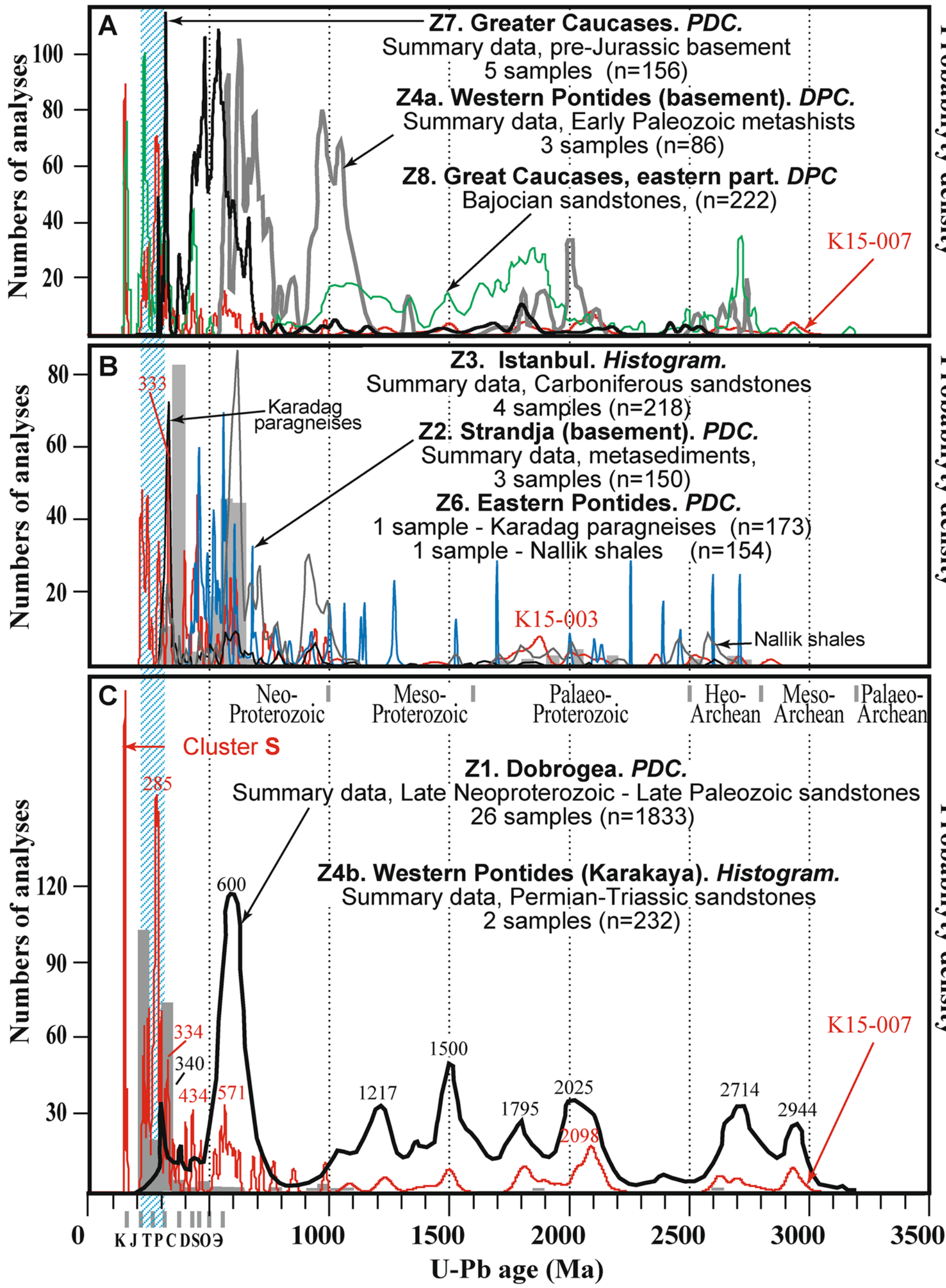

Fig. 7 Comparison of U–Pb ages of detrital zircons (with discordance ≤ 10%) from samples K15-007 **a**, **c** and K15-003 **b** with analogous data (some shown in the form of histograms, some in the form of *PDC*) for **BABSC**, (for location see Fig. 1). The strip of blue oblique shading under all diagrams corresponds to the Permian–Triassic time interval. **Z1. Dobrogea** (Balintoni and Balica 2016). **Z2. Strandja** (Sunal et al. 2008). **Z3. Istanbul.** Pontian flysch (Okay et al. 2011). **Z4a. Western Pontides.** Early Paleozoic metashists (the basement of Sakarya) (Ustaomer et al. 2012). **Z4b. Western Pontides.** Complex Karakaya (Ustaomer et al. 2016). **Z6. Eastern Pontides.** Karadag Paragneises and Nallick Shales (Ustaomer et al. 2013). **Z7. Great Caucasus.** Pre-Jurassic basement (Somin 2011). **Z8. Greater Caucasus, eastern part.** The Bajocian sandstones (Allen et al. 2006)

ancient Dobrogea (meta)sedimentary strata or their analogs. In contrast, a lack of Mesoproterozoic zircons in sample K15-003 (with only a single zircon of this age), makes contribution of the Dobrogea (meta)sediments to this sample highly improbable.

Strandja (Z2) According to Sunal et al. (2008), terranes comprising the Precambrian basement of the Strandja massif were rifted from Africa and were docked to Arct-Laurasia in vicinity of both the Armorica and Avalonia tectonic units of Western Europe. Available detrital zircon data (Sunal et al. 2008; Natal'in et al. 2012) for Paleozoic (430–315 Ma) sedimentary rocks sampling the Strandja basement record mixed sources with a prevalence of Ediacaran and younger zircon populations.

Only a few age peaks of the *PDC* from samples K15-007 (Figs. 7b, 9) and K15-003 (Fig. 7b) correlate with those in the spectrum of the Paleozoic sedimentary rocks of Strandja within the Cryogenic—Carboniferous time interval. Otherwise, a general difference in the zircon age spectra makes it unlikely that significant amounts of erosion products from the Strandja Paleozoic sedimentary rocks contributed to the Upper Jurassic conglomerates of the **MtCr**.

Istanbul (Z3) A study of detrital zircons from 4 Carboniferous sandstones (Pontian flysch) from the eastern part of the

Istanbul block (Okay et al. 2011) showed two major age populations (Fig. 7b) Carboniferous (390–335 Ma) and Cambrian–Ediacaran (640–520 Ma). Only a few zircons have Archean and Paleoproterozoic ages. Okay et al. (2011) suggested that (1) one source of detritus for the Pontian flysch was a Late Devonian—Early Carboniferous magmatic–metamorphic province formed on the Neoproterozoic basement and (2) the Istanbul terrane correlates with the Avalonian terranes of Central Europe, which collided with Armorican terranes in Carboniferous time.

In samples K15-007 and K15-003 only a few zircons of Carboniferous age were recorded (groups **D4** and **B3**, respectively). All these zircons have substantially negative ε_{Hf}, which indicates a Mesoproterozoic age of the protolith, at least 1.3 Ga. However, the zircons from the Pontian flysch, have Neoproterozoic model ages. These two observations make it unlikely that the Pontian flysch contributed significantly to the K15-007 and K15-003 samples.

Western Pontides, basement (Z4a) The dissimilarity of age distribution patterns of the detrital zircons from the basement of the Western Pontides (Ustaomer et al. 2012; Fig. 7b), excludes the Early Paleozoic schists of the Western Pontides as a significant secondary source of zircons for the K15-007 and K15-003 samples. However, minor contributions of their erosional products to the studied samples cannot be excluded.

Western Pontides, Karakay complex (Z4b) The U–Pb and Hf-isotope data for detrital zircons from 23 samples representing 6 formations of the Permian–Triassic complex of Karakay, which is treated as a Palaeo-Tethys subduction–accretion complex (Ustaomer et al. 2016), show an excellent correlation with zircons from samples K15-007 and K15-003 (Figs. 6b, 7a) over the 220–400 Ma time range. The zircons from the Karakaya complex with ages 300–500 Ma (including Carboniferous zircons) are characterized only by negative (including substantially negative) ε_{Hf}. Since only the substantially negative ε_{Hf} ($-2 \div -7$) in our samples are in Carboniferous zircons from groups **D4** and **B3**, the Karakay complex and its analogs must be regarded as a very possible secondary source of zircons in the Upper Jurassic conglomerates of **MtCr**.

Eastern Pontides (Z6) Detrital zircons from the Middle Devonian—Early Carboniferous Caragadi and Nallick shales (Ustaomer et al. 2013; Fig. 7b) show dominant populations with Late Neoproterozoic and Late Paleozoic ages and a complete absence of zircons with ages in the range 1.0–1.5 and 2.2–2.4 Ga. The pattern of age distribution for these two units varies somewhat in the age range of 0.6–1 Ga, but it is well matched in ages over 1 Ga and younger than 0.6 Ga. In general, for ages older than 500 Ma, there is a very good coincidence with the age spectra of K15-003 sample, especially the Early Proterozoic peak. Thus, some complexes in the Eastern Pontides with provenance signals similar to the Caragadi and Narlick shales represent a very plausible secondary source of zircons from the K15-003 sample site location.

The Greater Caucasus, Pre-Jurassic basement (Z7) According to the current interpretation of the paleogeographic situation at the end of the Jurassic (Figs. 3, 7b), the complexes of the Greater Caucasus could not be considered as a secondary source of zircons from the Upper Jurassic conglomerates of **MtCr**, since the products of their destruction could not reach the shelf of the Dobrogea–Crimea Uplift. However, the zircon data reported for this region by Somin (2011) are very important, since they recorded a large number of Permian and Early Triassic zircons. Until now, large-volume Triassic granite complexes have not been known from the Pontides or the Caucasus, and the question of the primary sources of Triassic zircons for **BABSC** is still open. The finding of significant amounts of Triassic zircons confirms the existence of a Triassic magmatic belt, the position of which is inferred to be in the basement of the Steppe Crimea and the Scythian platform (Fig. C5). The sedimentary sequences of the Greater Caucasus might be intermediate accumulators of Permian and Early Triassic zircons.

The Greater Caucasus, eastern part, Bajosian sandstones (Z8) The comparison with detrital zircons from the Bajosian sandstones in the eastern part of the Greater Caucasus (Fig. 7b) shows that there is no correlation between the provenance signal **Z7** from the pre-Jurassic basement of the Greater Caucasus and the provenance signal of **Z8**. This means that the studied Bajocian sandstones were derived from sources distinct from those of the pre-Jurassic basement of the Greater Caucasus, and are most likely products of the destruction of the Eastern Pontides. The Bajosian sandstones had been formed only 10–15 Ma before the accumulation of the Upper Jurassic conglomerates of **MtCr**. They contain numerous Middle Jurassic zircons (magmatism simultaneous with sedimentation) and a very prominent Late Triassic peak in *PDC*.

Taurides (Z12) According to Avigad et al. (2016), the Taurides block is underlain by the Late Neoproterozoic Cadomian basement, the provenance signal of which differs significantly from the Neoproterozoic Pan-African provenance signal of northeastern Africa (Fig. 8). Like other Cadomian terranes of Western Europe, the Taurides basement includes a greywacke sedimentary sequence of Middle–Late Ediacaran age deposited in a back-arc basin on the periphery of Afro-Arabia over a south-directed proto-Tethys subduction zone. The greywacke complex was deformed and metamorphosed to various degrees and was intruded by Late Ediacarian–Cambrian granites (Cadomian orogeny). In contrast to the ~ 300 Ma Neoproterozoic crustal evolution of Afro-Arabia, the Cadomian basement of the Taurides developed rapidly, over only ~ 50 Ma. The entire

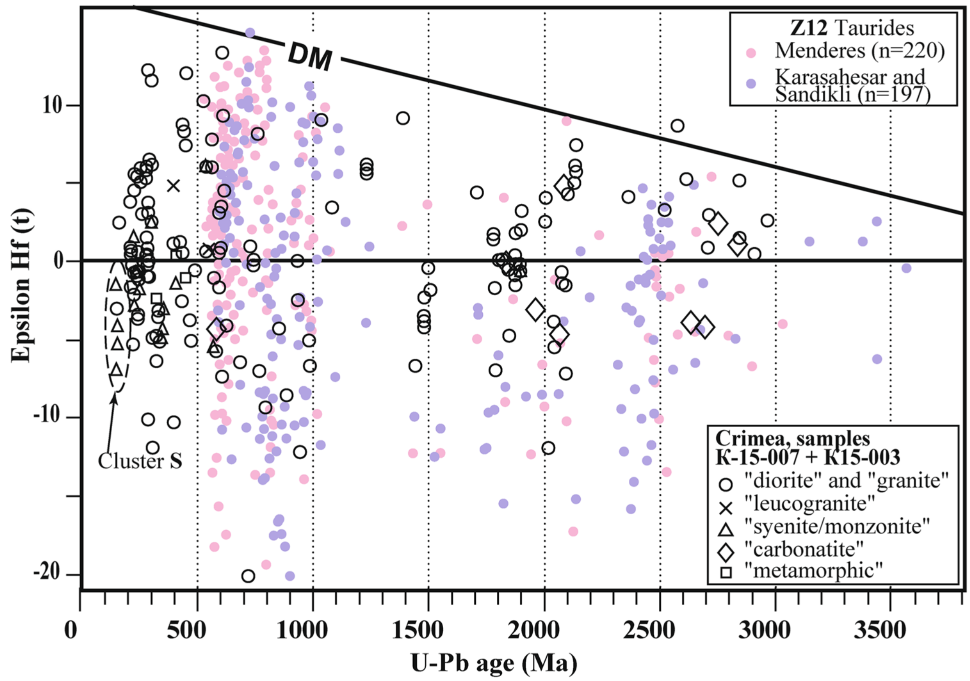

Fig. 8 Comparison of U–Pb and Lu–Hf isotope data for detrital zircons from samples K15-007 and K15-003 with analogous data for the Taurides zircons (**Z12**), according to (Avigad et al. 2016)

cycle of sedimentation, metamorphism, and magmatism in the Taurides basement occurred in the Latest Ediacaran—Cambrian, ending the formation of the Taurides basement. The sedimentary and meta-sedimentary complexes of the Taurides basement could be interpreted as an intermediate accumulator of the Mesoproterozoic and older zircons of Gondwanan affinity and their secondary source for the Pontides. In particular, the set of zircons from the Eastern Pontides with Precambrian ages (**Z6**) corresponds well to the provenance signal from the Menderes complex (Fig. 8).

Comparison with detrital zircons from the Late Jurassic and younger sediments of Crimea, Greater Caucasus, and Central Pontides

Crimea (Z0) U–Pb dating of detrital zircons from 9 samples from the Middle Jurassic–Neogene sandstones of the Southern coast of Crimea (Nikishin et al. 2015a) defines 3 prominent peaks with ages at 102, 170 and 280 Ma in *PDC* (total of 602 analyses) (Fig. 9). The peak at 280 Ma corresponds with peaks at 285 and 289 Ma obtained for samples K15-007 and K15-003, respectively. Secondary peaks in *PDC* formed by smaller numbers of analyses are defined at 10, 150, 247 and 325 Ma. The age distribution pattern is very similar to the K15-007 sample for data over 225 Ma, but significantly different in the age range from 150 to 225 Ma. A strong peak at ~ 170 Ma recorded in the Nikishin et al. (2015a) dataset corresponds to the ages of the Dzhidair intrusion and the Pervomaysky stock (Fig. C2). In sample K15-003, Jurassic zircons have not been identified, while in sample K15-007 they are represented only by the **D1** group.

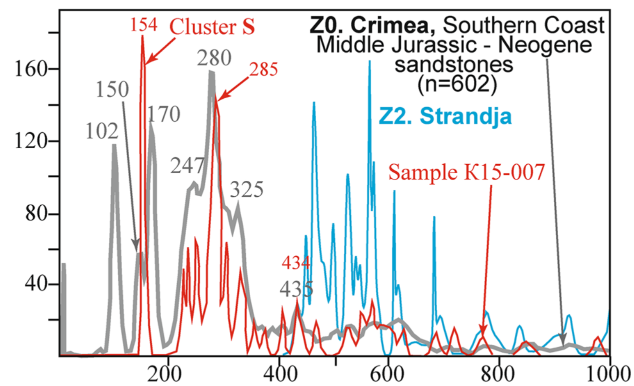

Fig. 9 Comparison of U–Pb ages of detrital zircons from the K15-007 sample and summary data for 9 samples of the Middle Jurassic–Neogene sandstones of the Southern coast of Crimea (**Z0**), according to (Nikishin et al. 2015a), as well as for the Strandja basement (**Z2**) according to (Sunal et al. 2008)

Central Pontides (Z5) Thirteen samples (1194 analyses) of detrital zircons from the Early Cretaceous turbidites of the Central Pontides (Okay et al. 2013; Akdogan et al. 2017) characterize in detail the arrival of detritus to the Early Cretaceous Caglayan basin (Fig. C7). In the Early Cretaceous this basin was located directly southward of the present-day **MtCr** (Figs. 1, 3), and its formation is certainly related to the initial stages of the subsidence of the Black Sea basin. The shelf where the conglomerates of the **MtCr** formed in the Upper Jurassic was the northern part of this basin at its earliest stages of development.

The provenance signals in the eastern and western parts of the basin are very different: in the eastern part, Archean and Paleoproterozoic zircons prevail in the detritus (61%), while Neoproterozoic and Carboniferous zircons (68%) dominate in the western part. According to Akdogan et al. (2017), detrital zircons in the central part of the basin show spectra resembling a mixture of zircons from the western and eastern parts. In addition, the central part of the basin is characterized by the presence of two very significant Late Triassic-age peaks (Fig. C7b), which are not manifested in the eastern, nor in the western part of the basin. These features of the age spectra of zircons from different parts of the Early Cretaceous Caglayan basin indicate extremely isolated and significantly different sources for the different parts of the Caglayan basin, and little mixing of the material in it. This situation is common in extensional structures at the initial stages, when systems of linear ridges and isolated graben basins are formed, as into the Basin and Range Province in the southwestern part of USA.

There are no Early Cretaceous or Jurassic zircons in the western part of the Caglayan basin (Fig. C7b) and this is similar to the K15-003 sample. However, in the central and eastern parts of the basin, Jurassic and Early Cretaceous zircons constitute about 2% of the total number of zircons, which is interpreted as reflecting the absence of simultaneous sedimentation and magmatism in the region (Akdoğan et al. 2017). This distribution is also similar in sample K15-007. The Jurassic and Lower Cretaceous zircons were most likely from small-volume local sources; they possibly originate from short-lived magmatic/metamorphic events (including underwater), confined to the walls of grabens.

The Greater Caucasus (Z9) The detrital zircon data from the Early Oligocene sandstones of the Maikop (Fig. C7) are presented as an evidence of the Permo-Triassic and Jurassic zircons in the **BABSC**.

Implications for paleogeographic reconstructions

Since the Us (and Sarmatian part of the EEP) is excluded as primary source and EEP as a secondary source of Archaean zircons, then the EEP also cannot be a source of Paleoproterozoic and Mesoproterozoic zircons. The latter are present in a limited amount in sample K15-007, but only a single zircon grain was found in sample K15-003. Since Mesoproterozoic zircons are rare in the Pontides deposits (where only single grains are found), but very common in the Late Neoproterozoic–Late Paleozoic complexes of Dobrogea (**Z1**), the most probable secondary source of the Mesoproterozoic zircons in the Upper Jurassic conglomerates in the sample K15-007 is the Dobrogea complexes. We pointed out that the Dobrogea complexes of the Late Neoproterozoic–Late Paleozoic age contain not only Mesoproterozoic zircons, but also Neoproterozoic, Paleoproterozoic and Archean zircons with ages that compare well to those found in the K15-007 sample (Fig. 7c). Recycling of detritus from the Late Neoproterozoic–Late Paleozoic Dobrogea complexes to the sample K15-007 can explain the zircons with Precambrian ages observed in this sample.

The age distribution of the Precambrian zircons from sample K15-003 is characterized by presence of the Early Neoproterozoic peak in *PDC*, of the Precambrian zircons from the sample K15-003 are perfectly comparable with those of the provenance signal **Z6**, Eastern Pontides (Fig. 7b).

Early and Middle Jurassic magmatism is widely manifested in the exposed rocks of the **MtCr** and the Pontides and actually, numerous Jurassic zircons of various ages are present in the younger sedimentary units of the Crimea (repeated recycling of zircons) as demonstrated previously (Nikishin et al. 2015a), where age peaks at about 150 and 170 Ma are evident (Fig. 9). In sample K15-007 Jurassic zircons are represented by only 5 grains at about 154 Ma (cluster **S**) and one with an age of 164 Ma (collectively—group **D1**). The next older zircon of 225 ± 4 Ma ($D = 4.78\%$) is already Triassic. In sample K15-003, the mean age of the two youngest zircons is ~ 215 Ma; this is also much older than the stratigraphic age of the Upper Jurassic conglomerates, which is at least 155 Ma. Thus, despite the wide representation of Jurassic magmatism in the **MtCr** and the Pontides, their detrital products are not recorded in the studied samples, except for the 6 zircons of group **D1** in the sample K15-007. This definitely shows that the zircons of cluster **S** originated from a very proximal and specific local source, which from all possible primary sources of Jurassic zircons only appeared in sample K15-007, while from other Jurassic sources of the **MtCr** and Pontides, zircons made it neither into K15- 007, nor into K15-003. Together with other very significant characteristics in the analysed detrital zircons, this implies that at the very end of Jurassic time the Upper Jurassic conglomerates, at least at the sampling sites, were situated along the paleo-coastline of the Dobrogea–Crimea Uplift.

The Upper Jurassic conglomerates at the K15-007 sampling site definitely could not be formed due to erosion of a single crustal block or a single stratum. In the conglomerates, zircons record a contribution of a closely located Late Jurassic magmatic complex (cluster **S**) and the erosion products of the Archean, Paleoproterozoic and Mesoproterozoic complexes from distant primary sources. This could occur only due to repeated recycling.

Paleogeographic reconstructions (Fig. 3), together with the analysis of the distribution of the crystalline complexes of different ages in the **BABSC** (Figs. C1–C6) allow us to conclude that the first-cycle zircons could only be grains from a nearby local source (group **D1**), and less likely, Triassic zircons (or some of them) from relics of magmatic/

metamorphic rocks of the proposed Triassic magmatic belt, which might be a part of the eroding Dobrogea–Crimea Uplift. If the crystalline complexes of the pre-Upper Jurassic basement of Crimea were brought to the erosion surface at the Dobrogea–Crimea Uplift in Upper Urassic time, the products of their erosion could have reached the shelf of the Dobrogea–Crimea Uplift and thus be incorporated into the Upper Jurassic conglomerates. All remaining zircons are definitely recycled grains.

To explain the presence of the observed zircons in sample K15-007, it is sufficient to mix the erosional products of the Late Neoproterozoic–Late Paleozoic meta-sedimentary complexes of Dobrogea (**Z1**) and Permian–Triassic sandstones of the Karakay complex or its analogs (**Z4b**), and to add 6 zircons from the local source (for group **D1**). Since the provenance signal of the Western Pontides (**Z4b)** contains minimal amounts of pre-Ordovician zircons, the total signal will retain all the features of the **Z1** age spectrum for pre-Ordovician ages. The signal (**Z4b**) will provide groups of zircons with Ordovician—Late Triassic ages. Since in the sample K15-007 the number of Triassic—Ordovician and all older zircons is approximately the same, then when mixed, the total amount of zircon from Dobrogea (**Z1**) should roughly correspond to the total number of all zircons from the Western Pontides (**Z4b)**. Thus, the recorded distribution of zircon in sample K15-007 can be explained by a single mixing episode with approximately equal proportions of zircons from the secondary sources of Dobrogea (**Z1**) and Western Pontides (**Z4b**) with the addition of 6 zircons (6dZr) from the local source (**D1**):

$$K15{-}007 \sim= 50\%(\mathbf{Z1}) + 50\%(\mathbf{Z4b}) + 6\mathbf{dZr}(\mathbf{D1})$$

To explain the distribution of the observed zircon in the sample K15-003, it is sufficient to mix the detrital material of the Eastern (**Z6**) and Western (**Z4b**) Pontides. However, since there is no clear separation in age between the provenance signals of the Eastern and Western Pontides, as between Dobrogea and the Western Pontides, we cannot estimate in what proportions mixing should occur. Thus, the recorded features of zircon in sample K15-003 can be explained by mixing zircons in some proportions from the secondary sources of the Eastern (x) % and (100 − x) % Western Pontides:

$$K15 - 003 \sim= x\%(\mathbf{Z6}) + (100 - x)\%(\mathbf{Z4b})$$

The proposed model for mixing zircons from these sources reproduces the following features of the zircon populations in the samples K15-007 and K15-003:

1. Representation of all populations of detrital zircons recorded in samples.
2. Differences in age groups in samples K15-007 and K15-003 for ages over 500 Ma and the similarity of age spectra for zircons younger than 400 Ma (in the time interval of the Triassic—Carboniferous).
3. Quantitative proportions between the Triassic—Ordovician and the rest of older zircons in sample K15-007.
4. Evolved Hf-isotope composition (negative $\varepsilon_{\mathrm{Hf}}$) of zircons with ages younger than Devonian.

In the proposed model, all zircons older than Late Neoproterozoic ultimately are not Baltic, but Gondwanan in origin. They have contributed to the Upper Jurassic conglomerates due to recycling from (meta)sedimentary complexes of terranes docked to Baltica at different times. At the same time, zircons in sample K15-007 originated from terranes with Amazonia affinity (recycled through Dobrogea), and zircons in sample K15-003 from terranes related to northeastern Africa and Arabia (recycling through Taurides).

The proposed model for mixing of the erosional products of complexes of the Crimea–Dobrogea Uplift and Pontides is consistent with the reconstructed change in the Late Jurassic paleogeographic situation within the **BABSC** (Fig. 3). In the Middle Jurassic basin, the detritus from the Pontides accumulated (Fig. 3a), while the products of the destruction of the Caucasus, the EEP and complexes in the **MtCr** that contain Lower and Middle Jurassic magmatic rocks, were not supplied to the basin. At places proximal to the future sampling sites K15-007 and K15-003, the detritus of the Western Pontides (signal **Z4b** from the Karakaya complex or its analogs) had arrived. At the K15-003 site the products of the destruction of the Eastern Pontides (signal **Z6** from Karadag Paragneises and Nallik shales or their analogs) were also available.

Then, at the very end of the Jurassic, the subsidence of the Pontides began (Fig. 3b). This inevitably caused an increase in the steepness of the shelf at the southern slope of the Dobrogea–Crimea Uplift and led to new influx of detritus from the Dobrogea–Crimea Uplift, starting to reach the interior regions of the basin more remote from the land. This made it possible to mix older and younger inputs. At the same time, paleotectonic reconstructions show that in the Latest Jurassic (Tithonian) the Central and Western Pontides ceased to erode and new detritus from Pontides most likely could not contribute to the sampling sites.

The small size of the Dobrogea–Crimea Uplift excludes the existence of a large river. Most likely a small river flowed in the intermontane valley, which was a continuation on land of the Sudak–Western-Caucasian turbidite trough. The river carried the erosional products of the Uplift to the nearest shelf areas. The sedimentary structures of the Upper Jurassic conglomerates suggest that the Demerzhi Fm. (near K15-007 sample site) accumulated on the shelf in the delta region of a small mountain river. This suggestion is supported by the fact that in the sample K15-007, the products of destruction of a specific magmatic body with an age of about 154 Ma were found, the magmatism of which was actually coeval with the formation of the conglomerates. The sampling site K15-003 was most likely located outside the unloading zone of the small river streams of the Dobrogea–Crimea Uplift, so the zircons from the Dobrogea–Crimea Uplift were not supplied to this site, where only recycling of the Jurassic deposits from the nearest local uplifts and mixing of the provenance signals Eastern and Western Pontides had occured.

The existing paleogeographic reconstructions do not contradict paleotectonic reconstructions, according to which the Jurassic volcanic arcs existed in the Eastern (Sen 2007; Rolland et al. 2009; Topuz et al. 2013a, b) and Central (Okay et al. 2014) Pontides. Relics of the Late Jurassic ophiolites and island arc granitoids are known in the Southern Apuseni Mountaintes (Gallhofer et al. 2016). In the Crimea, Lower and Middle Jurassic magmatism also is widely distributed (Fig. C5). Highly likely, these arcs were parts of the large complicated Jurassic–Cretaceous arc magmatic belt, whose relics are traced now from the Western Europe throughout northern parts of the Anatolian Peninsula and Lesser Caucasus into the northern Iran (Gallhofer et al. 2015).

In the Late Jurassic, the future Black Sea region underwent subsidence and stretching, accompanied by small-scale and short-duration magmatic/metamorphic events, while in the area of the Central Pontides, the uplifting quickly switched to subsidence, initiating the formation of the Lower Cretaceous Caglayan basin. However, there was no inversion in the most eastern parts of the Jurassic arc and elevated crustal blocks continued to exist. This is confirmed by the fact that in the Lower Cretaceous samples in the eastern part of the Caglayan basin, the proportion of ancient Precambrian detritus increased (Okay et al. 2013; Akdogan et al. 2017), suggesting that larger areas of the ancient basement or its cover complexes were brought up to the erosional surface. In the Early Cretaceous time, detritus supplied to the eastern part of the Caglayan basin contained substantial quantities of Paleoproterozoic and Archean zircons, but no Mesoproterozoic or Early Neoproterozoic material. However, this detritus did not reach the western part of the Caglayan basin, and Paleozoic detritus still dominated there.

Of course, the proposed model is idealized and represents an attempt to explain the results obtained for the samples K15-007 and K15-003 in the simplest possible way. However, the Mesozoic geodynamic history of the **BABSC** was extremely complex in space and time, and it is obvious that in reality a multi-stage and more complex scheme for the formation of provenance signals recorded in studied samples from a larger number of sources cannot be disregarded. A small part of the detritus in both samples, for example, could be recycled from the Strandja (**Z2**), Greater Caucasus (**Z7**) and/or the Central Pontides (**Z5**). Some of the zircons could be sourced not directly from the above-mentioned geological domains, but firstly into the Crimea Triassic flysch (Taurika Group or its analog) and from there into the shelf of the Dobrogea–Crimea Uplift. However, the established provenance from Dobrogea (**Z1**), Western (**Z4b**) and Eastern (**Z6**) Pontides in the samples K15-007 and K15-003 is beyond doubt.

Such a strong similarity of the Precambrian parts of the age spectra of the Dobrogea complexes (**Z1**) and the sample K15-007 cannot be a coincidence. Therefore, supported also by paleogeographic reconstructions, we believe that the products of erosion of the Dobrogea–Crimea Uplift complexes have contributed to the sample K15-007. The similarity of the provenance signals of the Precambrian parts of the K15-007 age spectra with the synthesis of data for 26 samples from the rocks of Late Neoproterozoic–Late Paleozoic age of Dobrogea indicate that in the Crimean part of the Dobrogea–Crimea Uplift (meta)sedimentary complexes, rather a crystalline basement, were predominantly eroded, because they have an identical provenance signal with the Dobrogea complexes. This is a strong evidence that in the Late Neoproterozoic and Paleozoic, (meta)sedimentary complexes, whose erosional products are present in sample K15-007, were formed uniformly and from similar feeding provinces and were part of the same complexes that now compose the Northern and Central Dobrogea. This in turn is an argument in favor of the similarity between the Crimea's Pre-Mesozoic foundation and the Dobrogea platform.

Conclusions

Comparison of the obtained geochronological results for zircons from samples K15-007 and K15-003 with known ages of the crystalline complexes of the **BABSC** and the available data for detrital zircons from (meta)sedimentary strata of different ages of the **BABSC**, reveal significant limitations on the interpretation of sources of zircons from the Upper Jurassic conglomerates of the **MtCr**.

A local source of rock types of alkaline affinities with U–Pb age of ~ 154 Ma and an at least Mesoproterozoic (T^{C}_{DM} = 1.1–1.6 Ga) model age has been established for one of the samples The probability of input of detritus from crystalline complexes of Sarmatian part of EEP into Upper Jurassic conglomerates, even through repeated recycling, is very insignificant. The zircons of the first cycle could only be from a local source and less likely the Triassic zircons (or some of them) from relics of the Triassic magmatic belt, which were part of the Dobrogea–Crimea Uplift at that time and thus could be eroded. The remaining older zircon populations are definitely recycled grains.

In the proposed model, all zircons from the studied samples that are older than Late Neoproterozoic have ultimately not Baltic, but Gondwanan origin. They have been introduced into Upper Jurassic conglomerates via recycling from the (meta)sedimentary complexes of terranes docked to the Baltica at different times (and then to Arct-Laurasia, when Baltica became a part of this supercontinent). The zircons in sample K15-007 were recycled through Dobrogea and originated from terranes with Amazonia affinity, and zircons in sample K15-003 were recycled through the Taurides and originated from terranes related to northeastern Africa and Arabia.

To explain the main isotopic (U–Pb and Hf isotopes) characteristics of the observed zircon populations in sample K15-007, it is sufficient to mix the erosional products of the Late Neoproterozoic–Late Paleozoic (meta)sediments of Dobrogea and Permian–Triassic Karakay complex or its analogs from Western Pontides, with the addition of some grains from a local source. In the sample K15-003, the contribution of the erosional products of Dobrogea–Crimea Uplift is very unlikely; the main supplying province apparently was the complexes of the Western and Eastern Pontides.

The strong similarity of the Precambrian parts of the age spectra of the Dobrogea complexes and the sample K15-007 suggests a resemblance of the Crimea's Pre-Mesozoic foundation and the Dobrogea platform.

Acknowledgements This study has been carried out following the plans of the scientific research of the IPE RAS. The analytical data were obtained using instrumentation funded by DEST Systemic Infrastructure Grants, ARC LIEF, NCRIS/Au Scope, industry partners and Macquarie University, and ARC FT110100-685 (Belousova E.A.) grant support. Handling of geochemical data, analysis processing, the regional gathering of geological materials, and publication preparation were executed with partial support from the RFBR (Grant 19-05-00284). This is contribution 1348 from the ARC Centre of Excellence for Core to Crust Fluid Systems (http://www.ccfs.mq.edu.au) and 1311 in the GEMOC Key Centre.

Funding IPE RAS (Federal basic funding). Macquarie University ARC FT110100-685 (Belousova E.A.). Russian Foundation Basic Research (Grant 19-05-00284) (Romanyuk T.V.).

References

Adamia S, Zakariadze G, Chkhotua T, Sadradze N, Tsereteli N, Chabukiani A, Gventsadze A (2011) Geology of the Caucasus: a review. Turk J Earth Sci. https://doi.org/10.3906/yer-1005-11

Akbayram K, Okay AI, Satir M (2013) Early Cretaceous closure of the Intra-Pontide Ocean in western Pontides (northwestern Turkey). J Geodyn. https://doi.org/10.1016/j.jog.2012.05.003

Akdoğan R, Okay AI, Sunal G, Tari G, Meinhold G, Kylander-Clark ARC (2017) Provenance of a large Lower Cretaceous turbidite submarine fan complex on the active Laurasian margin: central Pontides, Northern Turkey. J Asian Earth Sci. https://doi.org/10.1016/j.jseaes.2016.11.028

Allen MB, Morton AC, Fanning CM, Ismail-Zadeh AJ, Kroonenberg SB (2006) Zircon age constraints on sediment provenance in the Caspian region. J Geol Soc Lond. https://doi.org/10.1144/0016-764920-068

Avigad D, Abbo A, Gerdes A (2016) Origin of the Eastern Mediterranean: Neotethys rifting along a cryptic Cadomian suture with Afro-Arabia. Soc Am Bull, Geol. https://doi.org/10.1130/B31370.1

Balintoni I, Balica C (2016) Peri-Amazonian provenance of the Euxinic Craton components in Dobrogea and of the North Dobrogean Orogen components (Romania): a detrital zircon study. Precam Res. https://doi.org/10.1016/j.precamres.2016.03.008

Belousova EA, Walters S, Griffin WL, O'Reilly SY, Fisher NI (2002) Igneous zircon: trace element compositions as indicators of source rock type. Contrib Miner Petrol. https://doi.org/10.1007/s00410-002-0364-7

Belousova EA, Griffin WL, O'Reilly SY (2006) Zircon crystal morphology, trace element signatures and Hf isotope composition as a tool for petrogenetic modeling: examples from eastern Australian granitoids. J Petrol. https://doi.org/10.1093/petrology/egi077

Bogdanova SV, Bingen B, Gorbatschev R, Kheraskova TN, Kozlov VI, Puchkov VN, Volozh Y (2008) The East European Craton (Baltica) before and during the assembly of Rodinia. Precam Res. https://doi.org/10.1016/j.precamres.2007.04.024

Bozkurt E, Winchester JA, Yigitbas E, Ottley CJ (2008) Proterozoic ophiolites and mafic-ultramafic complexes marginal to the Istanbul Block: an exotic terrane of Avalonian afinity in NW Turkey. Tectonophysics. https://doi.org/10.1016/j.tecto.2008.04.027

Cavazza W, Roure FM, Spakman W, Stampfli GM, Ziegler PA (Eds) (2004) The TRANSMED Atlas: the Mediterranean Region from Crust to Mantle> Springer, Heidelberg, pp 141

Cavazza W, Federici I, Okay A, Zattin M (2012) Apatite fission-track thermochronology of the Western Pontides (NW Turkey). Geol Magazine. https://doi.org/10.1017/S0016756811000525

Celik OF, Marzoli A, Marschik R, Chiaradia M, Neubauer F, Oz I (2011) Early-Middle Jurassic intra-oceanic subduction in the Izmir-Ankara-Erzincan Ocean, Northern Turkey. Tectonophysics. https://doi.org/10.1016/j.tecto.2011.06.007

Chiu H-Y, Chung S-L, Zarrinkoub MH, Mohammadi SS, Khatib MM, Iizuka Y (2013) Zircon U–Pb age constraints from Iran on the magmatic evolution related to Neotethyan subduction and Zagros orogeny. Lithos. https://doi.org/10.1016/j.lithos.2013.01.006

Dokuz A (2011) A slab detachment and delamination model for the generation of Carboniferous high potassium I-type magmatism in the Eastern Pontides, NE Turkey: Köse composite pluton. Gondwana Res. https://doi.org/10.1016/j.gr.2010.09.006

Gallhofer D, von Quadt A, Peytcheva I, Schmid SM, Heinrich CA (2015) Tectonic, magmatic and metallogenic evolution of the Late Cretaceous Arc in the Carpathian-Balkan orogeny. Tectonics. https://doi.org/10.1002/2015TC003834

Gallhofer D, von Quadt A, Schmid SM, Guillong M, Peytcheva I, Seghedi I (2016) Magmatic and tectonic history of Jurassic ophiolites and associated granitoids from the South Apuseni Mountains (Romania). Swiss J Geosci. https://doi.org/10.1007/s00015-016-0231-6

Galoyan G, Rolland Y, Sosson M, Corsini M, Billo S, Verati C, Melkonyan R (2009) Geology, geochemistry and $^{40}Ar/^{39}Ar$ dating of Sevan ophiolites (Lesser Caucasus, Armenia): evidence for Jurassic back-arc opening and hot spot event between the South Armenian Block and Eurasia. J Asian Earth Sci. https://doi.org/10.1016/j.jseaes.2008.04.002

Genc SC (2004) A Triassic large igneous province in the Pontides, northern Turkey: geochemical data for its tectonic setting. J Asian Earth Sci. https://doi.org/10.1016/S1367-9120(03)00090-7

Georgiev S, von Quadt A, Heinrich CA, Peytcheva I, Marchev P (2012) Time evolution of a rifted continental arc: integrated ID-TIMS and LA-ICPMS study of magmatic zircons from the Eastern Srednogorie, Bulgaria. Lithos. https://doi.org/1016/j.lithos.2012.06.020

Goncuoglu MC, Gursu S, Tekin UK, Koksal S (2008) New data on the evolution of the Neotethyan oceanic branches in Turkey: late Jurassic ridge spreading in the Intra-Pontide branch. Ofioliti. https://doi.org/10.4454/ofioliti.v33i2.366

Goncuoglu MC, Marroni M, Sayit K, Tekin UK, Ottria G, Pandol L, Ellero A (2012) The Ayli Dag ophiolite sequence (central-northern Turkey): a fragment of Middle Jurassic oceanic lithosphere within the Intra-Pontide suture zone. Ofioliti. https://doi.org/10.4454/ofioliti.v37i2.407

Griffin WL, Pearson NJ, Belousova E, Jackson SE, O'Reilly SY, van Achterberg E, Shee SR (2000) The Hf isotope composition of cratonic mantle: LAM-MC-ICPMS analysis of zircon megacrysts in kimberlites. Geochim Cosmochim Acta. https://doi.org/10.1016/S0016-7037(99)00343-9

Griffin WL, Wang X, Jackson SE, Pearson NJ, O'Reilly SY, Xu X, Zhou X (2002) Zircon chemistry and magma genesis, SE China: in situ analysis of Hf isotopes, Pingtan and Tonglu igneous complexes. Lithos. https://doi.org/10.1016/S0024-4937(02)00082-8

Griffin WL, Belousova EA, Shee SR, Pearson NJ, O'Reilly SY (2004) Archean crustal evolution in the northern Yilgarn Craton: U–Pb and Hf-isotope evidence from detrital zircons. Precam Res. https://doi.org/10.1016/j.precamres.2003.12.011

Griffin WL, Belousova EA, Walters SG, O'Reilly SY (2006) Archean and Proterozoic crustal evolution in the Eastern Succession of the Mt Isa district, Australia: U–Pb and Hf-isotope studies of detrital zircons. Aust J Earth Sci 10:100. https://doi.org/10.1080/08120090500434591

Griffin WL, Belousova EA, O'Reilly SY (2007) TerraneChron Analysis of Zircons from Western Australian Samples Record. Geol. Survey of Western Australia. V.4

Henderson BJ, Collins WJ, Murphy JB, Gutierrez-Alonso G, Hand M (2016) Gondwanan basement terranes of the Variscan-Appalachian orogen: Baltican, Saharan and West African hafnium isotopic fingerprints in Avalonia, Iberia and the Armorican Terranes. Tectonophysics. https://doi.org/10.1016/j.tecto.2015.11.020

Hippolyte J-C, Müller C, Kaymakc N, Sangu E (2010) Dating of the Black Sea Basin: new nannoplankton ages from its inverted margin in the Central Pontides (Turkey). In: Sosson M, Kaymakci N, Stephenson RA, Bergerat F, Starostenko V (ed) Sedimentary basin tectonics from the Black Sea and Caucasus to the Arabian Platform. Geological Society London Special Publications, vol 340. https://doi.org/10.1144/SP340.7

Kroner U, Mansy J-L, Mazur S, Aleksandrowski P, Hann HP, Huckriede H, Lacquement F, Lamarche J, Ledru P, Pharao TC, Zedler H, Zeh A, Zulaf G (2008) Variscan tectonics. In: The Geology of Central Europe: Volume 1: Precam and Palaeozoic. Geological Society London, C11. 65p

Linnemann U, McNaughton NJ, Romer RL, Gehmlich M, Drost K, Tonk C (2004) West African provenance for Saxo-Thuringia (Bohemian Massif): did Armorica ever leave pre-Pangean Gondwana? U–Pb-SHRIMP zircon evidence and the Nd-isotopic record. Int J Earth Sci. https://doi.org/10.1007/s00531-004-0413-8

Linnemann U, Nance RD, Kraft P, Zulauf G (Eds.) (2007) The evolution of the Rheic Ocean: from Avalonian-Cadomian active margin to Alleghenian-Variscan collision. Geological Society of America Special Papers, vol 423. https://doi.org/10.1130/978-0-8137-2423-2.vii

Linnemann U, Ouzegane K, Drareni A, Hofmann M, Becker S, Gartner A, Sagawe A (2011) Sands of West Gondwana: an archive of secular magmatism and plate interactions—a case study from the Cambro-Ordovician section of the Tassili Ouan Ahaggar (Algerian Sahara) using U–Pb–LA–ICP–MS detrital zircon ages. Lithos. https://doi.org/10.1016/j.lithos.2011.01.010

Linnemann U, Gerdes A, Hofmann M, Marko L (2014) The Cadomian Orogen: neoproterozoic to Early Cambrian crustal growth and orogenic zoning along the periphery of the West African Craton—Constraints from U–Pb zircon ages and Hf isotopes (Schwarzburg Antiform, Germany). Precam Res. https://doi.org/10.1016/j.precamres.2013.08.007

Masse J-P, Tüysüz O, Fenerci-Masse M, Özer S, Sar B (2009) Stratigraphic organisation, spatial distribution, paleoenvironmental reconstruction, and demise of Lower Cretaceous (Barremian–lower Aptian) carbonate platforms of the Western Pontides (Black Sea region, Turkey). Cretaceous Res. https://doi.org/10.1016/j.cretres.2009.05.004

Meinhold G, Kostopoulos D, Frei D, Himmerkus F, Reischmann T (2010) U–Pb LA-SF-ICP-MS zircon geochronology of the Serbo-Macedonian Massif, Greece: palaeotectonic constraints for Gondwana-derived terranes in the Eastern Mediterranean. Int J Earth Sci (Geol Rundsch). https://doi.org/10.1007/s00531-009-0425-5

Meinhold G, Morton AC, Fanning CM, Frei D, Howard JP, Phillips RJ, Strogen D, Whitham AG (2011) Evidence from detrital zircons for recycling of Mesoproterozoic and Neoproterozoic crust recorded in Paleozoic and Mesozoic sandstones of southern Libya. Earth Planet Sci Lett. https://doi.org/10.1016/j.epsl.2011.09.056

Meinhold G, Morton AC, Avigad D (2013) New insights into peri-Gondwana paleogeography and the Gondwana super-fan system from detrital zircon U–Pb ages. Gondwana Res. https://doi.org/10.1016/j.gr.2012.05.003

Moghadam HS, Stern RJ, Kimura J-I, Hirahara Y, Sebda R, Miyazaki T (2012) Hf–Nd isotope constraints on the origin of Dehshir Ophiolite, Central Iran. Island Arc. https://doi.org/10.1111/j.1440-1738.2012.00815.x

Moghadam HS, Li X-H, Griffin WL, Stern RJ, Thomsen TB, Meinhold G, Aharipour R, O'Reilly SY (2017) Early Paleozoic tectonic reconstruction of Iran: tales from detrital zircon geochronology. Lithos. https://doi.org/10.1016/j.lithos.2016.09.008

Morag N, Avigad D, Gerdes A, Belousova E, Harlavan Y (2011) Crustal evolution and recycling in the northern Arabian–Nubian Shield: new perspectives from zircon Lu–Hf and U–Pb systematics. Precam Res. https://doi.org/10.1016/j.precamres.2011.01.004

Murphy JB, Nance RD (2008) The Pangea conundrum. Geology. https://doi.org/10.1130/G24966A.1

Murphy JB, Strachan RA, Nance RD, Parker KD, Fowler MB (2000) Proto-Avalonia: a 1.2–1.0 Ga tectonothermal event and constraints for the evolution of Rodinia. Geology. https://doi.org/10.1130/0091-7613(2000)28<1071:PAGTEA>2.0.CO;2

Murphy JB, Fernández-Suárez J, Keppie JD, Jeffries TE (2004a) Contiguous rather than discrete Paleozoic histories for the Avalon and Meguma terranes based on detrital zircon data. Geology. https://doi.org/10.1130/G20351.1

Murphy JB, Fernández-Suárez J, Jeffries TE, Strachan RA (2004b) U–Pb (LA–ICP–MS) dating of detrital zircons from Cambrian clastic rocks in Avalonia: erosion of a Neoproterozoic arc along the northern Gondwanan margin. J Geol Soc Lond. https://doi.org/10.1144/0016-764903-064

Murphy JB, Pisarevsky SA, Nance RD, Keppie JD (2004c) Neoproterozoic—Early Paleozoic evolution of peri-Gondwanan terranes: implications for Laurentia-Gondwana connections. Int J Earth Sci. https://doi.org/10.1007/s00531-004-0412-9

Nance RD, Gutierrez-Alonso G, Keppie JD, Linnemann U, Murphy BJ, Quesada C, Strachan RA, Woodcock NH (2013) A brief history of the Rheic Ocean. Geosci Front. https://doi.org/10.1016/j.gsf.2011.11.008

Natal'in B, Sunal G, Satir M, Toraman E (2012) Tectonics of the Strandja Massif, NW Turkey: history of a long-lived Arc at the Northern Margin of Palaeo-Tethys. Turk J Earth Sci. https://doi.org/10.3906/yer-1006-29

Nikishin AM, Ziegler PA, Bolotov SN, Fokin P (2011) Late Palaeozoic to Cenozoic evolution of the Black Sea-Southern Eastern Europe Region: a view from the Russian Platform. Turk J Earth Sci. https://doi.org/10.3906/yer-1005-22

Nikishin AM, Wannier M, Alekseev AS, Almendinger OA, Fokin PA, Gabdullin RR, Khudoley AK, Kopaevich LF, Mityukov AV, Petrov EI, Rubsova EV (2015a) Mesozoic to recent geological history of southern Crimea and the Eastern Black Sea region. In: Sosson M, Stephenson RA, Adamia SA (ed) Tectonic Evolution of the Eastern Black Sea and Caucasus. Geological Society London Special Publications, vol 428. https://doi.org/10.1144/SP428.1

Nikishin AM, Okay A, Tuysuz O, Demirer A, Wannier M, Amelin N, Petrov E (2015b) The Black Sea basins structure and history: new model based on new deep penetration regional seismic data. Part 1: Basins structure and fill. Mar Pet Geol. https://doi.org/10.1016/j.marpetgeo.2014.08.017

Nikishin AM, Okay A, Tuysuz O, Demirer A, Wannier M, Amelin N, Petrov E (2015c) The Black Sea basins structure and history: new model based on new deep penetration regional seismic data. Part 2: Tectonic history and paleogeography. Mar Pet Geol. https://doi.org/10.1016/j.marpetgeo.2014.08.018

Okay AI, Nikishin AM (2015) Tectonic evolution of the southern margin of Laurasia in the Black Sea region. Int Geol Rev. https://doi.org/10.1080/00206814.2015.1010609

Okay AI, Tüysüz O (1999) Tethyan sutures of northern Turkey. In: Durand B, Jolivet L, Horva TF, Seranne M (eds), The Mediterranean Basin: tertiary extension within the Alpine Orogen. Geological Society London Special Publications, vol 156. https://doi.org/10.1144/GSL.SP.1999.156.01.22

Okay AI, Tanzel I, Tüysüz O (2001) Obduction, subduction and collision as reflected in the Upper Cretaceous-Lower Eocene sedimentary record of Western Turkey. Geol Magz. https://doi.org/10.1017/S0016756801005088

Okay AI, Satir M, Siebel W (2006) Pre-Alpide Palaeozoic and Mesozoic orogenic events in the Eastern Mediterranean region. In: Gee DG, Stephenson RA (ed), European lithosphere dynamics, Geological Society London, Memoirs, vol 32. https://doi.org/10.1144/GSL.MEM.2006.032.01.23

Okay AI, Bozkurt E, Satir M, Yigitbas E, Crowley QG, Shang CK (2008) Defining the southern margin of Avalonia in the Pontides: geochronological data from the Late Proterozoic and Ordovician granitoids from NW Turkey. Tectonophysics. https://doi.org/10.1016/j.tecto.2008.02.004

Okay AI, Zattin M, Cavazza W (2010) Apatite fission track data for the Miocene Arabia-Eurasia collision. Geology. https://doi.org/10.1130/G30234.1

Okay N, Zack T, Okay AI, Barth M (2011) Sinistral transport along the Trans-European Suture Zone: Detrital zircon-rutile geochronology and sandstone petrography from the Carboniferous flysch of the Pontides. Geol Magz. https://doi.org/10.1017/S0016756810000804

Okay AI, Sunal G, Sherlock S, Altiner D, Tuysuz O, Kylander-Clark ARC, Aygul M (2013) Early Cretaceous sedimentation and orogeny on the southern active margin of Eurasia: Central Pontides, Turkey. Tectonics. https://doi.org/10.1002/tect.20077

Okay AI, Sunal G, Tuysuz O, Sherlock S, Keskin M, Kylander-Clark ARC (2014) Low-pressure—high temperature metamorphism during extension in a Jurassic magmatic arc, Central Pontides, Turkey. J Metamorphic Geol. https://doi.org/10.1111/jmg.12058

Okay AI, Altiner D, Kilic AM (2015) Triassic limestone, turbidite and serpentinite—Cimmeride orogeny in the Central Pontides. Geol Magz. https://doi.org/10.1017/S0016756814000429

Okay AI, Altiner D, Sunal G Aygül M, Akdoğan R, Altinerand S, Simmons M (2018) Geology of evolution of the Central Pontides. In: Simmons MD, Tari GC, Okay AI (ed) Petroleum Geology of the Black Sea, Geological Society London Special Publications, vol 464. https://doi.org/10.1144/SP464.3

Peytcheva I, von Quadt A, Georgiev N, Ivanov Z, Heinrich CA, Frank M (2008) Combining trace-element compositions, U–Pb geochronology and Hf isotopes in zircons to unravel complex calcalkaline magma chambers in the Upper Cretaceous Srednogorie zone (Bulgaria). Lithos. https://doi.org/10.1016/j.lithos.2008.01.004

Rolland Y, Galoyan G, Bosch D, Sosson M, Corsini M, Fornari M, Verati C (2009) Jurassic back-arc and hot-spot related series in the Armenian ophiolites—implications for the obduction process. Lithos. https://doi.org/10.1016/j.lithos.2009.02.006

Saintot A, Stephenson RA, Stovba S, Brunet MF, Yegorova T, Starostenko V (2006) The evolution of the southern margin of Eastern Europe (Eastern European and Scythian platforms) from the latest Precambrian-Early Palaeozoic to the Early Cretaceous. In: Gee DG, Stephenson RA (eds) European lithosphere dynamics: London, Geological Society, Memoirs 32, pp 481–505. https://doi.org/10.1144/GSL.MEM.2006.032.01.30

Samson SD, Dlemos RS, Miller BV, Hamilton MA (2005) Neoproterozoic palaeogeography of the Cadomia and Avalon terranes: constraints from detrital zircon U–Pb ages. J Geol Soc Lond. https://doi.org/10.1144/0016-764904-003

Sayit K, Goncuoglu MC, Furman T (2010) Petrological reconstruction of Triassic seamounts/oceanic islands within the Palaeotethys: geochemical implications from the Karakaya subduction/accretion Complex, Northern Turkey. Lithos. https://doi.org/10.1016/j.lithos.2010.08.004

Schmid SM, Bernoulli D, Fügenschuh B, Matenco L, Schefer S, Schuster R, Tischler M, Ustaszewski K (2008) The Alpine-Carpathian-Dinaridic orogenic system: correlation and evolution of tectonic units. Swiss J Geosci. https://doi.org/10.1007/s00015-008-1247-3

Seghedi A (2012) Palaeozoic formations from Dobrugea and Pre-Dobrugea—an overview. Turk J Earth Sci. https://doi.org/10.3906/yer-1101-20

Sen C (2007) Jurassic volcanism in the Eastern Pontides: is it rift related or subduction related? Turk J Earth Sci 16(4):523–539

Shumlyanskyy L, Hawkesworth C, Dhuime B, Billstrom K, Claesson S, Storey C (2015) $^{207}Pb/^{206}Pb$ ages and Hf isotope composition of zircons from sedimentary rocks of the Ukrainian shield: crustal growth of the south-western part of East European craton from Archaean to Neoproterozoic. Precam Res. https://doi.org/10.1016/j.precamres.2015.01.007

Solov'ev AV, Rogov MA (2010) First fission-track dating of zircons from Mesozoic complexes of the Crimea. Stratigr Geol Correlat. https://doi.org/10.1134/S0869593810030068

Somin M (2011) Pre-Jurassic basement of the Greater Caucasus: brief overview. Turk J Earth Sci. https://doi.org/10.3906/yer-1008-6

Stampfli GM, Borel GD (2002) A plate tectonic model for the Paleozoic and Mesozoic constrained by dynamic plate boundaries and restored synthetic oceanic isochrones. Earth Planet Sci Lett. https://doi.org/10.1016/S0012-821X(01)00588-X

Stampfli G, Kozur HW (2006) Europe from Variscan to Alpine cycles. In: Gee DG, Stepherson R (eds), European Lithosphere Dynamics. Geological Society London, Memoirs, 32. https://doi.org/10.1144/GSL.MEM.2006.032.01.04

Stampfli GM, Von Raumer JF, Borel GD (2002) Paleozoic evolution of pre-Variscan terranes: from Gondwana to the Variscan collision. In: Martinez CJR, Hatcher Jr RD, Arenas R, Diaz Garcia F (eds) Variscan-Appalachian dynamics: The building of the Late Palaeozoic basement. Geological Society of America Special Papers, 364. https://doi.org/10.1130/0-8137-2364-7.263

Stampfli GM, Hochard C, Verard C, Wilhem C, von Raumer J (2013) The formation of Pangea. Tectonophysics. https://doi.org/10.1016/j.tecto.2013.02.037

Starostenko V, Janik T, Yegorova T, Farfuliak L et al (2015) Seismic model of the crust and upper mantle in the Scythian Platform: the DOBRE-5 profile across the north western Black Sea and the Crimean Peninsula. Geophys J Int. https://doi.org/10.1093/gji/ggv018

Strachan RA, Linneman U, Jeffries T, Drost K, Ulrich J (2014) Armorican provenance for melange deposits below the Lizard ophiolite (Cornwall, UK)—evidence for Devonian obduction of Cadomian and Lower Palaeozoic crust onto the southrn margin of Avalonia. Int J Earth Sci. https://doi.org/10.1007/s00531-013-0961-x

Sunal G, Satir M, Natal'in B, Toraman E (2008) Paleotectonic position of the Strandja Massif and surrounding continental blocks based on zircon Pb–Pb age studies. Int Geol Rev. https://doi.org/10.2747/0020-6814.50.6.519

Teipel U, Eichhorn R, Loth G, Rohrmuller J, Holl R, Kennedy A (2004) U–Pb SHRIMP and Nd isotopic data from the western Bohemian Massif (Bayerischer Wald, Germany): implications for Upper Vendian and Lower Ordovician magmatism. Int J Earth Sci. https://doi.org/10.1007/s00531-004-0419-2

Topuz G, Celik OF, Sengor AMC, Altintas IE, Zack T, Rolland Y, Barth M (2013a) Jurassic ophiolite formation and emplacement as backstop to a subduction-accretion complex in northeast Turkey, the Refahiye ophiolite, and relation to the Balkan ophiolites. Am J Sci. https://doi.org/10.2475/10.2013.04

Topuz G, Gocmengil G, Rolland Y, Celik OF, Zack T, Schmitt AK (2013b) Jurassic accretionary complex and ophiolite from northeast Turkey: no evidence for the Cimmerian continental ribbon. Geology. https://doi.org/10.1130/G33577.1

Ustaomer PA, Ustaomer T, Gerdes A, Zulauf G (2011) Detrital zircon ages from Ordovician quartzites of the Istanbul exotic terrane (NW Turkey): evidence for Amazonian affinity. Int J Earth Sci. https://doi.org/10.1007/s00531-010-0539-9

Ustaomer PA, Ustaomer T, Robertson AHF (2012) Ion Probe U–Pb dating of the Central Sakarya basement: a peri-Gondwana terrane intruded by late Lower Carboniferous subduction/collision related granitic rocks. Turk J Earth Sci. https://doi.org/10.3906/yer-1103-1

Ustaomer T, Robertson AHF, Ustaomer PA, Gerdes A, Peytcheva I (2013) Constraints on Variscan and Cimmerian magmatism and metamorphism in the Pontides (Yusufeli -Artvin area), NE Turkey from U–Pb dating and granite geochemistry. In: Robertson AHF, Parlak O, Unlugenc UC (Eds) Geol. development of Anatolia and the easternmost Mediterranean region. Geological Society London Special Publications, vol 372. https://doi.org/10.1144/SP372.13

Ustaomer PA, Ustaomer T, Robertson AHF, Gerdes A (2016) Implications of U–Pb and Lu–Hf isotopic analysis of detrital zircons for the depositional age, provenance and tectonic setting of the Permian-Triassic Palaeotethyan Karakaya Complex, NW Turkey. Int J Earth Sci 10:100. https://doi.org/10.1007/s00531-015-1225-8

von Raumer JF, Bussy F, Schaltegger U, Schulz B, Stampfl GM (2013) Pre-Mesozoic Alpine basements—their place in the European Paleozoic framework. GSA Bull. https://doi.org/10.1130/B30654.1

Yılmaz A, Adamia S, Yılmaz H (2014) Comparisons of the suture zones along a geotraverse from the Scythian Platform to the Arabian Platform. Geosci Front 5(6):855–875. https://doi.org/10.1016/j.gsf.2013.10.004